Georgia Institute of Technology
DANIEL GUGGENHEIM SCHOOL OF AERONAUTICS
Atlanta, Georgia

GEORGIA TECH
RECEIVED
MAY 23 1962
LIBRARY

PROJECT NO. 159

A BLADE ELEMENT ANALYSIS FOR LIFTING ROTORS THAT IS APPLICABLE FOR LARGE INFLOW AND BLADE ANGLES AND ANY REASONABLE BLADE GEOMETRY

By

WALTER CASTLES, JR. AND NOAH C. NEW

- o - o - o - o - o - o - o - o - o - o -

CONTRACT NO. NAw-5906

NATIONAL ADVISORY COMMITTEE FOR AERONAUTICS

- o - o - o - o - o - o - o - o - o - o -

MAY, 1951

Georgia Institute of Technology
DANIEL GUGGENHEIM SCHOOL OF AERONAUTICS
Atlanta, Georgia

PROJECT NO. 159

A BLADE ELEMENT ANALYSIS FOR LIFTING ROTORS THAT IS APPLICABLE FOR LARGE INFLOW AND BLADE ANGLES AND ANY REASONABLE BLADE GEOMETRY

By

WALTER CASTLES, JR. AND NOAH C. NEW

- o - o - o - o - o - o - o - o - o - o -

CONTRACT NO. NAw-5906

NATIONAL ADVISORY COMMITTEE FOR AERONAUTICS

- o - o - o - o - o - o - o - o - o - o -

MAY, 1951

A BLADE ELEMENT ANALYSIS FOR LIFTING ROTORS THAT IS APPLICABLE FOR LARGE INFLOW AND BLADE ANGLES AND ANY REASONABLE BLADE GEOMETRY.

Prepared by:

Walter Castles, Jr., Assoc. Prof.
Daniel Guggenheim School of
Aeronautics

Approved by:

Donnell W. Dutton, Director
Daniel Guggenheim School of
Aeronautics

Released by:

Gerald A. Rosselot, Director
State Engineering Experiment
Station

May, 1951

TABLE OF CONTENTS

A BLADE ELEMENT ANALYSIS FOR LIFTING ROTORS THAT IS APPLICABLE FOR LARGE INFLOW AND BLADE ANGLES AND ANY REASONABLE BLADE GEOMETRY

By Walter Castles, Jr. and Noah C. New

Daniel Guggenheim School of Aeronautics
Georgia Institute of Technology

SUMMARY

Simple approximate solutions are derived for the relationships between the rotor thrust and flight-path velocity components and the rotor torque and in-plane forces. These approximate solutions, based upon the assumption of a triangular distribution of blade circulation and a linear variation of blade-element profile drag with lift, are sufficiently accurate for performance estimation and the determination of the equilibrium angle of attack and lateral tilt of the tip-path plane.

A set of more exact blade-element equations are then derived giving the relations between the thrust and flight-path velocity components and the equilibrium blade angles, torque, and in-plane forces and moments. Neither the blade element nor the approximate solutions are dependent upon the usual approximations that the inflow angle, ϕ , and blade angle, θ , of the blade elements are small angles. Thus the present equations should be useful for convertaplane as well as helicopter calculations.

It appears that nonlinear blade twist may be desirable for a convertaplane rotor in order to obtain useful propeller efficiencies. Therefore, the blade-element equations have been arranged so that any reasonable distribution of blade twist may be used. Also, the equations were set up

in terms of an arbitrary blade-chord distribution since it was found that the use of the actual blade-chord distribution and the elimination of the usual assumption that the blade airfoil extended inboard to the axis of rotation largely eliminated the necessity for the usual reverse-flow corrections. Tables of the necessary factors are included for blades having a linear taper, linear twist, and an airfoil contour from r = 0.15 R to r = R, and for blades having a linear taper, helical twist, and airfoil contours extending from r = 0.20 R to r = R.

The present analysis is based upon the following approximations:

1. The blade-element lift coefficient may be assumed to be proportional to the sine of the blade-element angle of attack, and the blade-element profile drag coefficient may be represented by the first three terms of a Fourier series in the blade-element angle of attack.

2. The blade axes may be assumed to be, and to remain, straight lines.

3. The lateral and longitudinal variations of the normal component of the induced velocity at the tip-path plane may be assumed to be linear.

4. The effects of compressibility on the tip sections of the advancing blade may be neglected.

5. The radial and tangential components of the induced velocity may be neglected.

6. Blade tip effects may be neglected.

A comparison of the results given by the present equations with the full-scale helicopter test data of reference 1 shows that the equations are of useful accuracy for the helicopter flight range covered in that reference. At the present time there are no experimental data available to check the accuracy of the equations in the convertaplane flight range.

INTRODUCTION

This project, sponsored by the National Advisory Committee for Aeronautics and the Georgia Tech Engineering Experiment Station, was undertaken in order to develop a blade-element analysis for lifting rotors that would be useful for convertaplane as well as helicopter calculations. This necessitated the elimination of the usual approximations that the blade-element inflow angle, ϕ , and the blade angle, θ , are small angles and required a reasonably exact treatment of the blade geometry.

It was found that the small angle approximations could be eliminated for the lift forces by writing the lift coefficient of the blade element as

$$c_l = a \sin \alpha_r = a(\sin \theta_r \cos \phi_r + \cos \theta_r \sin \phi_r)$$

and, consequently, the thrust component of force, $dL \cos \phi_r$, on a blade element as

$$dL \cos \phi_r = \tfrac{1}{2} \rho a (U \cos \phi_r)[\sin \theta_r (U \cos \phi_r) + \cos \theta_r (U \sin \phi_r)] c \, dr$$

since $U \cos \phi_r$ and $U \sin \phi_r$, the in-plane and normal components of velocity at the blade element perpendicular to the blade axis and measured with respect to the tip-path plane, can be simply expressed in reasonably exact form. Similarly, the tangential component of the lift on a blade element may be expressed as

$$dL \sin \phi_r = \tfrac{1}{2} \rho a (U \sin \phi_r)[\sin \theta_r (U \cos \phi_r) + \cos \theta_r (U \sin \phi_r)] c \, dr$$

It was also found that the small angle approximations could be largely eliminated and a considerable simplification effected for the helicopter flight conditions by expressing the blade-element profile drag coefficient,

c_{d_o} , as

$$c_{d_o} = \varepsilon_o + \varepsilon_1 \sin\alpha_r + \varepsilon_2 \cos\alpha_r$$

It follows that

$$dD_o \cos\phi_w = \tfrac{1}{2}\rho c\, dr \Big\{ \varepsilon_o (U\cos\phi_w)^2 \sqrt{1 + \left(\frac{U\sin\phi_w}{U\cos\phi_w}\right)^2}$$

$$+ \varepsilon_1 (U\cos\phi_w)\left[\sin\theta_w (U\cos\phi_w) + \cos\theta_w (U\sin\phi_w)\right]$$

$$+ \varepsilon_2 (U\cos\phi_w)\left[\cos\theta_w (U\cos\phi_w) - \sin\theta_w (U\sin\phi_w)\right]\Big\}$$

where the radical, $\sqrt{1 + \left(\frac{U\sin\phi_w}{U\cos\phi_w}\right)^2}$, may be approximated by the first two terms of its binomial expansion.

For the more severe convertaplane flight conditions, considerable error is introduced by dropping third and higher terms of the binomial expansion, since ε_o is of the order of 0.50 for the three term approximation. Thus, for those flight conditions where $|\lambda_w| > 0.10$ it becomes more accurate to use the two-term approximation for the profile drag coefficient, $c_{d_o} = \varepsilon_1 \sin\alpha_r + \varepsilon_2 \cos\alpha_r$ for which the geometry is "exact". This is permissible since the relative effects of the profile drag become less important as the propeller condition is approached.

The exact blade geometry has been retained throughout by expressing the blade-chord and blade-twist distribution in the form of the following constants:

$$\sigma_n = \frac{1}{\pi R}\int_{x_1}^{1} c\, x^{n-1}\, dx$$

$$\sigma_{nc} = \frac{1}{\pi R}\int_{x_1}^{1} c \cos\theta_t\, x^{n-1}\, dx$$

and $$\sigma_{ns} = \frac{1}{\pi R}\int_{x_1}^{1} c \sin\theta_t\, x^{n-1}\, dx$$

where θ_t = blade twist in the angle of zero lift between the reference station and nondimensional radius, x .

Values of these constants are given in tables 4, 5, and 6 for blades having linear taper, linear twist and $x_1 = 0.15$ and for blades having linear taper, helical twist and $x_1 = 0.20$.

The present system of equations has been set up with respect to tip-path-plane coordinates or coordinates based on the virtual axis of rotation rather than the usual coordinate system based on the plane of zero feathering in order to obtain shorter expressions for the in-plane rotor forces and moments. The use of coordinates aligned with the virtual axis of rotation also facilitates the treatment of some accelerated flight problems.

Certain refinements in the induced velocity theory, as given in reference 2, have been incorporated with some minor changes in the present equations along with the necessary terms for an arbitrary angular velocity of roll and pitch of the tip-path plane.

Standard N.A.C.A. nomenclature has been used where possible, with the subscript, $\sim$, for virtual axis of rotation appended to the usual symbols

which, in this paper, have a similar meaning but different numerical values.

NOTATION

(Note: All angles are in radian measure)

a slope of lift curve for blade element at 0.75 R (per radian)

a_0 rotor coning angle

$\bar{a}_0$ coning angle for zero blade-root bending moment

a_1 the coefficient of the sine component of the blade-cyclic-pitch angle measured with respect to the tip-path plane where

$$\theta_r = A_0 + \theta_t - a_1 \sin\psi + b_1 \cos\psi$$

also the coefficient of the cosine term of the Fourier series for the blade-flapping angle, β, measured with respect to the plane of zero feathering where

$$\beta = a_0 - a_1 \cos\psi - b_1 \sin\psi - a_2 \cos 2\psi - b_2 \sin 2\psi - \cdots$$

a_2 coefficient of the second harmonic cosine term in a Fourier series for the blade-flapping angle

A_0 mean blade-pitch angle at reference station, positive above tip-path plane.

b number of blades in rotor

b_1 coefficient of the cosine component of the blade-cyclic-pitch angle measured with respect to the tip-path plane,

also coefficient of the sine term of the Fourier series for the blade-flapping angle measured with respect to the plane of zero feathering

b_2 coefficient of the second harmonic sine term in the Fourier series for the blade-flapping angle

c blade chord at radius, r

c_o extended blade-root chord at r = 0 (for linear taper)

c_{d_o} section profile-drag coefficient

c_ℓ section-lift coefficient

C_{mx} rotor rolling-moment coefficient measured about X axis

$$\left(C_{mx} = \frac{M_x}{\frac{1}{2}\rho\pi\Omega^2R^5}\right)$$

C_{my} rotor pitching-moment coefficient measured about Y axis

$$\left(C_{my} = \frac{M_y}{\frac{1}{2}\rho\pi\Omega^2R^5}\right)$$

C_Q rotor torque coefficient $\left(C_Q = \frac{Q}{\rho\pi\Omega^2R^5}\right)$

C_T rotor thrust coefficient $\left(C_T = \frac{T}{\rho\pi\Omega^2R^4}\right)$

C_x rotor X-force coefficient $\left(C_x = \frac{F_x}{\frac{1}{2}\rho\pi\Omega^2R^4}\right)$

C_{xy} rotor-blade tangential force coefficient $\left(C_{xy} = \frac{F_{xy}}{\frac{1}{2}\rho\pi\Omega^2R^4}\right)$ positive in direction of rotation

C_y rotor Y-force coefficient $\left(C_y = \frac{F_y}{\frac{1}{2}\rho\pi\Omega^2R^4}\right)$

C_z rotor-blade thrust force coefficient $\left(C_z = \frac{F_z}{\frac{1}{2}\rho\pi\Omega^2R^4}\right)$

E_o mean blade-drag angle positive in the direction of rotation and measured between the blade axis and line through rotor axis of rotation and drag hinge.

(i.e. blade-drag angle, ζ , is $\zeta = E_o + E_1\cos\psi + F_1\sin\psi + \cdots$

E_1 coefficient of cosine term in expression for blade-drag angle

F_1 coefficient of sine term in expression for blade-drag angle

F_x component of rotor resultant force acting along X axis

F_{xy} tangential component of the resultant air force on a blade, positive in direction of rotation.

F_y component of rotor resultant force acting along Y axis.

F_z Z component of the resultant air force on a blade

g acceleration of gravity

h distance between longitudinal fuselage axis taken through c.g. and rotor hub, measured along the normal to the fuselage axis.

I_1 mass moment of inertia of a blade about the flapping hinge.

I_{nc} $\sigma_{nc} \sin A_o + \sigma_{ns} \cos A_o$

I_{ns} $\sigma_{ns} \sin A_o - \sigma_{nc} \cos A_o$

I_v mass moment of inertia of rotor about virtual axis of rotation

I_ζ mass moment of inertia of a blade about the drag hinge.

k_{a_o} blade-root spring constant (blade-root bending moment in foot pounds divided by angular deflection in radians of 3/4 R point from $\bar{a}_o$)

Q rotor torque, negative in direction of rotation

r radius of blade element, c dr

$\bar{r}$ radius of blade c.g.

r_β radius of flapping hinge

R radius of blade tip

t $\frac{\text{tip chord}}{c_o} - 1$ (for linearly tapered blades)

T rotor thrust, component of rotor resultant force along Z axis

U component of the resultant velocity at a blade element that is normal to the blade axis

v mean normal component of the induced velocity at the tip-path plane (positive down and to the rear)

V velocity along flight path

V_i Z component of the induced velocity at r, ψ, (positive in the $+Z$ direction)

w nondimensional slope of the longitudinal induced velocity variation

W gross weight plus down component of any acceleration force acting on aircraft

x nondimensional blade radius, $\frac{r}{R}$

x_1 nondimensional radius of inboard blade airfoil element

y nondimensional slope of the lateral induced velocity variation

α_f angle of attack of fuselage measured between flight-path velocity vector and longitudinal fuselage axis

α_r blade-element angle of attack measured from line of zero lift

α_v angle of attack of the tip-path plane measured in the X-Z plane between the flight-path velocity vector and the tip-path plane, positive below tip-path plane

β blade-flapping angle at azimuth angle,

(for tip-path plane $\beta_w = a_0 - a_2 \cos 2\psi - b_2 \sin 2\psi - \cdots$)

(for plane of zero feathering

$$\beta = a_0 - a_1 \cos\psi - b_1 \sin\psi - a_2 \cos 2\psi - b_2 \sin 2\psi - \cdots)$$

Γ circulation of a blade element at radius, r , and azimuth angle, ψ

Γ_0, Γ_1 constants in expression for Γ where $\Gamma = (\Gamma_0 + \Gamma_1 \sin\psi)x$

δ_0 value of c_{d_0} at $c_\ell = 0$

ε constant in linear approximation for c_{d_0} (i.e. $c_{d_0} = \delta_0 + \varepsilon c_\ell$)

$\varepsilon_0, \varepsilon_1, \varepsilon_2$ constants for first three terms of Fourier series expressing the relation between c_{d_0} and α_r (i.e. $c_{d_0} = \varepsilon_0 + \varepsilon_1 \sin\alpha_r + \varepsilon_2 \cos\alpha_r$ or $c_{d_0} = \varepsilon_1 \sin\alpha_r + \varepsilon_2 \cos\alpha_r$

ζ blade-drag angle at azimuth angle, ψ , positive in direction of rotation

θ_1 twist in zero-lift chord line between axis of rotation and blade tip for blades with linear twist, positive for increased angle at tip (i.e. $\theta_t = \theta_1 x$)

θ_t twist in rotor-blade angle of zero lift between reference station and radius, r , positive for larger angle outboard

θ_T design helix angle at tip of blade for blades with helical twist

θ_w pitch angle of blade element at radius, r , and azimuth angle, ψ , measured between zero-lift chord line and tip-path plane, positive above tip-path plane ($\theta_w = A_0 + \theta_t - a_1 \sin\psi + b_1 \cos\psi$)

θ_χ angular displacement of tip-path plane about X axis from horizontal

θ_y angular displacement of tip-path plane about Y axis from horizontal

λ_v inflow-velocity ratio at center of tip-path plane

$$\left(\lambda_v = \frac{V \sin \alpha_v - v}{\Omega R}\right)$$

μ_v in-plane velocity ratio at tip-path plane

$$\left(\mu_v = \frac{V \cos \alpha_v}{\Omega R}\right)$$

σ_n $\frac{1}{\pi R}\int_{x_1}^{1} c\, x^{n-1}\, dx$, (constants which express the blade-chord distribution)

(i.e. $\sigma_1 = \frac{1}{\pi R}\int_{x_1}^{1} c\, dx$

$\sigma_2 = \frac{1}{\pi R}\int_{x_1}^{1} c\, x\, dx$ etc.)

σ_{nc} $\frac{1}{\pi R}\int_{x_1}^{1} c \cos \theta_t\, x^{n-1}\, dx$

σ_{ns} $\frac{1}{\pi R}\int_{x_1}^{1} c \sin \theta_t\, x^{n-1}\, dx$ (constants which express the blade-chord and twist distribution)

ϕ_c angle between flight path and horizontal, positive below horizontal

ϕ_v inflow angle at blade element measured in a plane perpendicular to blade axis and between tip-path plane and relative wind, positive below tip-path plane.

ψ azimuth angle of blade axis measured about Z axis from X axis (Note: This angle is very nearly but not identically equal to the equivalent angle in the plane of zero feathering.)

ω_x angular velocity of roll of tip-path plane about X axis

ω_y angular velocity of pitch of tip-path plane about Y axis

Ω mean angular velocity of rotor-blade axis about Z axis

ANALYSIS AND DISCUSSION

Value of the Normal Component of the Induced Velocity at Radius, r, and Azimuth Angle, ψ.

It is shown in reference 2 that for a lightly loaded single rotor composed of a large number of blades, b, each having a circulation given by the expression

$$\Gamma = \Gamma_0 + \Gamma_1 \sin \psi \tag{1}$$

the mean value of the normal component of the induced velocity is

$$\nu = \frac{\frac{1}{2} \Omega R \, C_T}{\left(1 - \frac{3}{2} \mu_\nu^2\right) \sqrt{\lambda_\nu^2 + \mu_\nu^2}} \tag{2}$$

Equation 2 was derived on the assumption that the wake extended to infinity and had the form of a straight elliptic cylinder. Thus, for those flight conditions where a "vortex ring" type flow exists, equation 2 is not applicable and the value of ν must, at present, be obtained from experiment. The term $\left(1 - \frac{3}{2} \mu_\nu^2\right)$ in the denominator of equation 2 arises from the lateral dissymmetry in the blade circulation that is required for rolling moment equilibrium, and this term is the only correction which the elementary theory makes in Glauert's original hypothesis that $\nu = T/2\rho A V'$

If the distribution of the normal component of the induced velocity, V_i, over the tip-path plane be denoted by a power series in the non-dimensional radius, χ, and a Fourier series in the azimuth angle, ψ, such that for the first order terms

$$\frac{V_i}{\Omega R} = -\frac{\nu}{\Omega R} + w \chi \cos\psi + y \chi \sin\psi \qquad (3)$$

it can be shown from the results of reference 2 that

$$w \approx -\frac{4}{3}\left[(1-1.8\mu_\nu^2)\sqrt{1+\left(\frac{\lambda_\nu}{\mu_\nu}\right)^2} - \sqrt{\left(\frac{\lambda_\nu}{\mu_\nu}\right)^2}\right]\frac{\nu}{\Omega R} \qquad (4)$$

and

$$y \approx 2\mu_\nu \frac{\nu}{\Omega R} \qquad (5)$$

For level flight and $\mu_\nu > 0.15$ the expression for y may be simplified to

$$y \approx C_T \qquad (6)$$

It may be noted that for a pair of equally loaded, coaxial, counter-rotating rotors, the values of w and y are

$$w \approx -\frac{4}{3}\left[\sqrt{1+\left(\frac{\lambda_\nu}{\mu_\nu}\right)^2} - \sqrt{\left(\frac{\lambda_\nu}{\mu_\nu}\right)^2}\right]\frac{\nu}{\Omega R} \qquad (7)$$

and $y = 0 \qquad (8)$

Approximate Values of the Rotor Torque, X Force, and Y Force Coefficients

It is convenient for performance estimation and checking, and necessary, in the general case, for the determination of the angle of attack

and lateral tilt of the tip-path plane, to have expressions of useful accuracy for the rotor torque, X force, and Y force that are independent of the rotor-blade angles. One such set of equations which take into account all the principal variables may be obtained from a consideration of the distribution of the blade circulation. It may be noted before proceeding that the major part of the rotor torque and X force, which arises from the component of velocity normal to the tip-path plane acting on that large portion of the blade circulation which does not vary with azimuth angle, is independent of the radial distribution of the blade circulation for constant thrust and only a function of the magnitude and distribution of the inflow velocity. Consequently, since the magnitude and distribution of the inflow velocity are fixed by the flight-path velocity, angle of attack of the tip-path plane, and the assumptions as to the magnitude and distribution of the induced velocity, any reasonable approximation for the radial and azimuth distributions of the blade circulation, Γ , at radius, r , and azimuth angle, ψ , should give useful results. A triangular distribution of Γ along the radius and a sinusoidal variation with azimuth angle would appear to be a reasonable approximation. Then

$$\Gamma = (\Gamma_0 + \Gamma_1 \sin\psi)\chi \tag{9}$$

and the rotor thrust, T , is

$$T = \frac{\rho b}{2\pi R}\int_0^{2\pi}\int_0^{R} U\cos\phi_w\,(\Gamma_0 + \Gamma_1\sin\psi)\,r\,d\psi\,dr \tag{10}$$

But $$U\cos\phi_v = \Omega R(\chi + \mu_v \sin\psi) \tag{11}$$

or $$C_T = \frac{b}{\pi\Omega R^2}\left(\frac{\Gamma_0}{3} + \frac{\Gamma_1\mu_v}{4}\right) \tag{12}$$

Similarly the rotor rolling moment, M_x , which must be approximately equal to zero for unaccelerated flight, is

$$M_x = \frac{\rho b}{2\pi R}\int_0^{2\pi}\int_0^R U\cos\phi_v(\Gamma_0 + \Gamma_1\sin\psi)r^2\sin\psi\,d\psi\,dr \tag{13}$$

or for $M_x = 0$

$$\Gamma_1 = -\frac{4}{3}\Gamma_0\mu_v \tag{14}$$

and from equations 12 and 9

$$\Gamma = \frac{3\pi\Omega R^2 C_T}{b(1-\mu_v^2)}\left(1 - \frac{4}{3}\mu_v\sin\psi\right)\chi \tag{15}$$

The value of the blade element profile drag coefficient, c_{d_o} , may be represented with sufficient accuracy by two terms of a power series in the blade-element lift coefficient, c_ℓ , such that

$$c_{d_o} = \delta_o + \varepsilon c_\ell \tag{16}$$

where δ_o and ε are determined from the values of c_{d_o} at say $c_\ell = 0$ and $c_\ell = 0.7$.

Then the rotor torque, Q , is

$$Q = -\frac{\rho b}{2\pi}\int_0^{2\pi}\int_0^R U \sin\phi_w \Gamma r \, d\psi \, dr$$

$$+ \frac{\rho b \varepsilon}{2\pi}\int_0^{2\pi}\int_0^R U \cos\phi_w \Gamma r \, d\psi \, dr$$

$$+ \frac{\rho b \delta_0}{4\pi}\int_0^{2\pi}\int_0^R U^2 \cos\phi_w c r \, d\psi \, dr \cdot \qquad (17)$$

But $$U\sin\phi_w = \Omega R\left[\lambda_w + (\mu x - a_0\mu_w)\cos\psi + \eta x \sin\psi\right] \qquad (18)$$

Thus

$$C_Q = \frac{C_T\left(\frac{1}{2}\eta\mu_w - \lambda_w + \frac{3}{4}\varepsilon - \frac{2}{3}\varepsilon\mu_w^2\right)}{1-\mu_w^2}$$

$$+ \frac{1}{2} b \delta_0\left[\sigma_4 + \frac{1}{2}\left(\lambda_w^2 + \mu_w^2\right)\sigma_2\right] \qquad (19)$$

where $$\sigma_n = \frac{1}{\pi R}\int_{x_1}^{1} c\, x^{n-1} dx$$

For linearly tapered blades the values of σ_n may be obtained by interpolation from table 1. Similarly the rotor X and Y forces are

$$F_x = -\frac{\rho b}{2\pi}\int_0^{2\pi}\int_0^R U \sin\phi_w \Gamma \sin\psi \, d\psi \, dr$$

$$+ \frac{\rho b \varepsilon}{2\pi}\int_0^{2\pi}\int_0^R U \cos\phi_w \Gamma \sin\psi \, d\psi \, dr$$

$$+ \frac{\rho b \delta_0}{4\pi}\int_0^{2\pi}\int_0^R U^2 \cos\phi_w c \sin\psi \, d\psi \, dr \qquad (20)$$

and

$$F_y = \frac{\rho b}{2\pi}\int_0^{2\pi}\int_0^R U \sin\phi_w \Gamma \cos\psi \, d\psi \, dr$$

$$- \frac{\rho b \varepsilon}{2\pi}\int_0^{2\pi}\int_0^R U \cos\phi_w \Gamma \cos\psi \, d\psi \, dr$$

$$- \frac{\rho b \delta_0}{4\pi}\int_0^{2\pi}\int_0^R U^2 \cos\phi_w c \cos\psi \, d\psi \, dr \qquad (21)$$

and the values of the coefficients are

$$C_x = \frac{F_x}{\frac{1}{2}\rho\pi\Omega^2 R^4} = \frac{C_T(2\lambda_w\mu_w - \gamma + \frac{1}{6}\varepsilon\mu_w)}{1-\mu_w^2} + b\delta_0\mu_w\sigma_2 \qquad (22)$$

and

$$C_y = \frac{F_y}{\frac{1}{2}\rho\pi\Omega^2 R^4} = \frac{C_T(\mu_w - \frac{3}{2}a_0\mu_w)}{1-\mu_w^2} \qquad (23)$$

where

$$a_0 \approx \frac{\pi \rho R^5 C_T (\sigma_4 + \frac{1}{2}\mu_v^2 \sigma_2)}{b I_1 \sigma_3}$$

Equations 19, 22, and 23 for the torque, X-force, and Y-force coefficients should yield useful results provided there are no large areas of the rotor outside the reverse-flow region where the blade elements are stalled. It will be noted that the lateral induced-velocity variation has a relatively large effect on the magnitude of the X force. Table 2 shows a comparison of the calculated rotor torque coefficients and tip-path plane angles of attack, calculated from the X-force coefficients given by the above approximate equation, with the experimental values of reference 1 having $C_T \approx .00545$. Table 2 also shows a comparison of the values of C_X and C_y calculated from the above equations with the more exact values from the blade-element equations derived in later sections.

Determination of the Angle of Attack and Lateral Tilt of the Tip-Path Plane.

Given the flight path velocity, V , climb angle, ϕ_c , gross weight and vertical component of the inertia force, W , fuselage and wing drag, lift, moment characteristics, and position of center of gravity: the fuselage angle of attack and thus the fuselage and wing lift, L_F , and drag, D_F , can be obtained for the trim condition by setting the summation of moments, acting on the fuselage and wing and taken about the rotor hub, equal to zero. Since the lateral tilt of the tip-path plane has a negligible effect, it follows from the geometry of the above forces, as shown in figure 2, that

$$\tan \theta_y = - \frac{D_F \cos \phi_c - L_F \sin \phi_c + F_x \cos \theta_y}{W - L_F \cos \phi_c - D_F \sin \phi_c + F_x \sin \theta_y} \tag{24}$$

is a good approximation for unaccelerated flight. In general, the terms involving F_x will have only a small effect on the value of θ_y and a sufficiently exact solution can be obtained on the second iteration. Thus, as a first approximation,

$$\tan \theta_y = - \frac{D_F \cos \phi_c - L_F \sin \phi_c}{W - L_F \cos \phi_c - D_F \sin \phi_c} \tag{25}$$

$$\alpha_v = \phi_c + \theta_y \tag{26}$$

$$C_T = \frac{W - L_F \cos \phi_c - D_F \sin \phi_c}{\rho \pi \Omega^2 R^4 \cos \theta_y} \tag{27}$$

$$\mu_v = \frac{V \cos \alpha_v}{\Omega R} \tag{28}$$

$$\lambda_v = \frac{V \sin \alpha_v}{\Omega R} - \frac{v}{\Omega R} \tag{29}$$

The values of $\frac{v}{\Omega R}$ may be obtained from equation 2 or by double interpolation from table 3 which includes the experimental values for vertical descent from reference 3 and estimates of the values for the

inclined flight "vortex ring" states. The values of w , y , and F_x can then be determined from equations 4, 5, and 22, and from these the second approximations to the values of θ_{1y} , α_{nv} , and μ_{nv} can be made from equations 24, 26, and 28. If necessary, a new value of C_T may then be obtained from the equation

$$C_T = \frac{W - L_F \cos\phi_c - D_F \sin\phi_c + F_x \sin\theta_{1y}}{\rho\pi\Omega^2 R^4 \cos\theta_{1y}} \qquad (30)$$

and thus the more exact value of λ_{nv} from equation 29.

For helicopter calculations the first approximation for C_T is sufficiently accurate, and if μ_{nv} is small (i.e. $\mu_{nv} < 0.15$) the effect of F_x on α_{nv} may be neglected for level flight.

The tail-rotor thrust, T_T , required for a helicopter with a single main rotor is

$$T_T = \frac{Q}{\ell} \qquad (31)$$

where ℓ = perpendicular distance between axis of main and tail rotors and the value of C_Q may be obtained from equation 19. The lateral tilt, θ_x , of the tip-path plane for a single-rotor aircraft in unaccelerated flight is thus

$$\theta_x \approx \frac{\pm C_y + C_Q \frac{R}{\ell}}{C_T} \qquad (32)$$

where C_y is given by equation 23.

The Application of Two-Dimensional Airfoil Theory and Data to Rotor-Blade-Element-Calculations.

Two-dimensional thin-airfoil theory demonstrates that

$$c_\ell = a \sin \alpha \tag{33}$$

For a two-dimensional cascade of airfoils, equation 33 is modified by a multiplying function of the solidity, chord spacing, and blade angles that is very nearly unity for average lifting-rotor configurations as shown in reference 4. Thus, within the approximation that the radial components of flow may be neglected, equation 33 should be applicable for blade-element rotor theory over the unstalled range of blade-element angles of attack. Beyond the stall, equation 33 is somewhat less in error than the usual relation, $c_\ell = a\alpha$, as can be seen from figure 3 which is a plot of the above expressions and the experimental values of c_ℓ versus α for a NACA 0015 airfoil. The use of equation 33, rather than the usual approximation that $c_\ell = a\alpha$, allows the thrust and tangential components of lift on a blade element to be exactly expressed, within the approximations involved in neglecting radial components of the flow, in terms of the easily integrated in-plane and normal components of the velocity at the blade element, $U \cos \phi_w$, and $U \sin \phi_w$. Thus the usual approximation that the inflow angle, ϕ_w, is a small angle may be eliminated. This may be demonstrated as follows:

Omitting the negligible component of the profile drag, the thrust, dT, on a blade element, $c\,dr$, is

$$dT = \tfrac{1}{2} \rho U^2 c\, c_\ell \cos \phi_w \, dr \tag{34}$$

or since

$$c_l = a \sin\alpha_r = a(\sin\theta_{nr}\cos\phi_{nr} + \cos\theta_{nr}\sin\phi_{nr}) \tag{35}$$

$$dT = \tfrac{1}{2}\rho a c (U\cos\phi_{nr})\left[\sin\theta_{nr}(U\cos\phi_{nr}) + \cos\theta_{nr}(U\sin\phi_{nr})\right]dr \tag{36}$$

The tangential component of the lift on a blade element may be similarly expressed as

$$dL\sin\phi_{nr} = \tfrac{1}{2}\rho a c (U\sin\phi_{nr})\left[\sin\theta_{nr}(U\cos\phi_{nr}) + \cos\theta_{nr}(U\sin\phi_{nr})\right]dr \tag{37}$$

The value of the slope of the lift curve, a , of the blade-element airfoil in the above relations may be taken as the value corresponding to the Reynolds number, Mach number and surface roughness existing at the 3/4-radius point of the rotor blades under consideration. For the usual tip speeds, in the 500-feet-per-second range, the Prandtl-Glauert Mach number correction

$$a = \frac{a'}{\sqrt{1 - M^2}} \tag{38}$$

where a' = low Mach number lift-curve slope from two-dimensional wind tunnel tests

M = freestream Mach number at 3/4-blade radius

may be used to correct the lift-curve slope from low Mach number data.

The values of c_{d_o} obtained from two-dimensional wind tunnel tests at appropriate Reynolds numbers and model surface roughness should be directly applicable to rotor-blade-element calculations in the unstalled range of angles of attack below the Mach numbers and angles of attack

for drag divergence, since the effect of subsonic Mach number on profile drag is negligible as shown in reference 5. However, the two-dimensional values of c_{d_0} in the high angle-of-attack range around $\alpha = 90^\circ$ should probably be reduced from values of the order of 1.8 to values of the order of 1.2 due to the narrow span of the high angle-of-attack regions of the rotor blade and the equalizing effects of spanwise flow on the normal pressures. This effect may be seen in the variation of the drag coefficient of flat plates normal to the flow from a value of 2.0 for the two-dimensional plate down to about 1.4 for the square plate.

In view of the errors in the magnitude and distribution of the blade circulation that arise from the necessary neglect of blade deflections, etc., it is probably not justifiable to take into account secondary effects of the profile drag. Thus, expressing the relation between the profile-drag coefficient and the blade-element angle of attack by the first three terms of a Fourier series gives

$$c_{d_0} = \varepsilon_0 + \varepsilon_1 \sin\alpha_r + \varepsilon_2 \cos\alpha_r \qquad (39)$$

The constants in the above equation may be evaluated from the two-dimensional wind tunnel data for the blade airfoil at say $\alpha = 0^\circ$, 5°, and 10°. The advantages of equation 39 over the usual expression,

$$c_{d_0} = \delta_0 + \delta_1 \alpha_r + \delta_2 \alpha_r^2$$

are: the latter two terms of equation 39 can be exactly expressed in the known velocity components $U\cos\phi_w$ and $U\sin\phi_w$; the resulting expressions for the forces and moments on the blade are considerably

simplified by the absence of the squared term in α_r ; and it is an equally accurate approximation to the experimental values of c_{d_o} as may be seen from figure 4 (page). However, in using equation 39 it may be noted that the calculated value of c_{d_o} is the small difference between large quantities and thus the values of ε_o , ε_1 , and ε_2 , should be determined to four places in order to obtain the value of c_{d_o} to the customary accuracy. For the more severe convertaplane flight conditions where the inflow velocity is large ($|\lambda_w| > 0.10$) a certain error arises in the treatment of the ε_o terms, and it is necessary to fall back on the two-term approximation for c_{d_o} , $c_{d_o} = \varepsilon_1 \sin\alpha_r + \varepsilon_2 \cos\alpha_r$, where ε_1 and ε_2 are evaluated from the experimental data at say $\alpha = 2^\circ$ and $\alpha = 7^\circ$. This additional approximation is permissible for these flight conditions, since the relative effects of the profile drag become less important as the inflow velocities and rotor blade angles increase. For example, in propeller calculations the single point approximation, $c_{d_o} = \varepsilon_2$, is usually used.

It follows from the geometry and equations 35 and 39 that the tangential component of the profile drag on a blade element may be expressed as

$$dD_o \cos\phi_w = \tfrac{1}{2}\rho c (U\cos\phi_w)\Big\{\varepsilon_o U + \varepsilon_1\big[(U\cos\phi_w)\sin\theta_w + (U\sin\phi_w)\cos\theta_w\big] + \varepsilon_2\big[(U\cos\phi_w)\cos\theta_w - (U\sin\phi_w)\sin\theta_w\big]\Big\} dr \qquad (40)$$

Thrust of a Blade at Azimuth Angle, ψ

The thrust, F_z , of a blade at azimuth angle, ψ , is

$$F_z = \frac{1}{2}\rho a \int_{R_1}^{R} c(U\cos\phi_w)\left[(U\cos\phi_w)\sin\theta_w + (U\sin\phi_w)\cos\theta_w\right] dr \qquad (41)$$

In the general case it follows from the geometry that

$$U\cos\phi_w = \Omega R(x + \mu_w \sin\psi) \qquad (42)$$

and $$U\sin\phi_w = \Omega R\left[\lambda_w + (\omega x + \omega_y x - a_0\mu_w)\cos\psi\right.$$

$$+ (y - \omega_x)x\sin\psi + 2b_2 x\cos 2\psi$$

$$\left. - 2a_2 x\sin 2\psi \right] \qquad (43)$$

where ω_x = angular velocity of tip-path plane about x axis

ω_y = angular velocity of tip-path plane about y axis.

Neglecting the higher harmonics of the cyclic pitch that may arise from control system linkages, the pitch angle, θ_w , of a blade element ar radius, r , and azimuth angle, ψ , measured with respect to the tip-path plane, is

$$\theta_w = A_0 + \theta_t - a_1\sin\psi + b_1\cos\psi \qquad (44)$$

where A_o = mean blade-pitch angle at reference station.

θ_t = twist in rotor-blade angle of zero lift between reference station and radius, r .

a_1 = minus the coefficient of the sine component of the blade cyclic-pitch angle measured with respect to the tip-path plane.

b_1 = coefficient of the cosine component of the cyclic-pitch angle measured with respect to the tip-path plane.

In the general case (i.e. for the convertaplane) A_o and θ_t may not be small angles. However, it appears that the magnitude of the cyclic-pitch angle will always be limited by tip stall on the retreating blade to the range where it is a good approximation that

$$\sin(-a_1 \sin\psi + b_1 \cos\psi) = -a_1 \sin\psi + b_1 \cos\psi \tag{45}$$

and $$\cos(-a_1 \sin\psi + b_1 \cos\psi) = 1 \tag{46}$$

It follows from equation 44, upon expanding the functions sin θ_w and cos θ_w , that

$$\sin\theta_w = [\sin A_o + \cos A_o(-a_1 \sin\psi + b_1 \cos\psi)]\cos\theta_t$$

$$+[\cos A_o - \sin A_o(-a_1 \sin\psi + b_1 \cos\psi)]\sin\theta_t \tag{47}$$

$$\cos\theta_N = \left[\cos A_0 - \sin A_0 (-a_1 \sin\psi + b_1 \cos\psi)\right] \cos\theta_t$$

$$- \left[\sin A_0 + \cos A_0 (-a_1 \sin\psi + b_1 \cos\psi)\right] \sin\theta_t \qquad (48)$$

Substituting the values of $U\cos\phi_N$, $U\sin\phi_N$, $\sin\theta_N$ and $\cos\theta_N$ from equations 42, 43, 47, and 48, in equation 41, defining

$$\sigma_{nc} = \frac{1}{\pi R} \int_{x_1}^{1} c\, x^{n-1} \cos\theta_t \, dx \qquad (49)$$

$$\sigma_{ns} = \frac{1}{\pi R} \int_{x_1}^{1} c\, x^{n-1} \sin\theta_t \, dx \qquad (50)$$

$$I_{nc} = \sigma_{nc} \sin A_0 + \sigma_{ns} \cos A_0 \qquad (51)$$

$$I_{ns} = \sigma_{ns} \sin A_0 - \sigma_{nc} \cos A_0 \qquad (52)$$

and multiplying out the terms and reducing the functions of ψ to harmonic form gives for the thrust coefficient, $C_z = \frac{F_z}{\frac{1}{2}\rho\pi\Omega^2 R^4}$ of one blade at an azimuth angle, ψ, the expression of equation 53:

$C_z/a =$ Equation 53

	I_{3C}	I_{2C}	I_{1C}	I_{3S}	I_{2S}	I_{1S}
1	$1+\frac{1}{2}a_1(\gamma-\omega_x)$ $-\frac{1}{2}b_1(\omega+\omega_y)$	$\frac{1}{2}(a_0+a_2)b_1\mu_\nu$ $-\frac{1}{2}a_1b_2\mu_\nu$	$\frac{1}{2}(a_1\lambda_\nu+\mu_\nu)\mu_\nu$	$\frac{1}{2}(a_1a_2+b_1b_2)(\omega+\omega_y)$ $+\frac{1}{2}(a_1b_2-a_2b_1)(\gamma-\omega_x)$	$a_1\mu_\nu-\lambda_\nu$ $-\frac{1}{2}(\gamma-\omega_x)\mu_\nu$ $-\frac{1}{2}(a_1a_2+b_1b_2)a_0\mu_\nu$	
sin ψ	$a_2(b_1+\omega+\omega_y)$ $-b_1(a_1-\gamma+\omega_x)$	$(2-a_0a_2)\mu_\nu+a_1\lambda_\nu$ $+\frac{3}{4}a_1(\gamma-\omega_x)\mu_\nu$ $-\frac{1}{4}b_1(\omega+\omega_y)\mu_\nu$	$\frac{1}{4}a_0b_1\mu_\nu^2$	$a_1-(\gamma-\omega_x)$	$(a_1b_2-a_2b_1)\lambda_\nu$ $+b_2\mu_\nu$	$(\frac{3}{4}a_1\mu_\nu-\lambda_\nu)\mu_\nu$
cos ψ	$-a_2(a_1-\gamma+\omega_x)$ $-b_2(b_1+\omega+\omega_y)$	$a_0b_2\mu_\nu-b_1\lambda_\nu$ $+\frac{1}{4}a_1(\omega+\omega_y)\mu_\nu$ $-\frac{1}{4}b_1(\gamma-\omega_x)\mu_\nu$	$-\frac{1}{4}a_0a_1\mu_\nu^2$	$-b_1-(\omega+\omega_y)$	$(a_0+a_2)\mu_\nu$ $+(a_1a_2+b_1b_2)\lambda_\nu$	$-\frac{1}{4}b_1\mu_\nu^2$
sin 2ψ	$-\frac{1}{2}a_1(\omega+\omega_y)$ $-\frac{1}{2}b_1(\gamma-\omega_x)$	$-(\frac{1}{2}a_0+a_2)a_1\mu_\nu$ $+2a_2\lambda_\nu$	$-\frac{1}{2}b_1\lambda_\nu\mu_\nu$	$2a_2$ $+a_1a_2(\gamma-\omega_x)$ $-a_2b_1(\omega+\omega_y)$	$(a_0a_2-1)b_1\mu_\nu$ $-\frac{1}{2}(\omega+\omega_y)\mu_\nu$	$\frac{1}{2}a_0\mu_\nu^2$
cos 2ψ	$-\frac{1}{2}a_1(\gamma-\omega_x)$ $-\frac{1}{2}b_1(\omega+\omega_y)$	$(\frac{1}{2}a_0b_1+a_1b_2)\mu_\nu$ $-2b_2\lambda_\nu$	$-\frac{1}{2}(a_1\lambda_\nu+\mu_\nu)\mu_\nu$	$-2b_2$ $-a_1b_2(\gamma-\omega_x)$ $+b_1b_2(\omega+\omega_y)$	$-(a_1+a_0b_1b_2)\mu_\nu$ $+\frac{1}{2}(\gamma-\omega_x)\mu_\nu$	
sin 3ψ		$-\frac{1}{4}a_1(\gamma-\omega_x)\mu_\nu$ $-\frac{1}{4}b_1(\omega+\omega_y)\mu_\nu$	$\frac{1}{4}a_0b_1\mu_\nu^2$			$-\frac{1}{4}a_1\mu_\nu^2$
cos 3ψ		$-\frac{1}{4}a_1(\omega+\omega_y)\mu_\nu$ $+\frac{1}{4}b_1(\gamma-\omega_x)\mu_\nu$	$\frac{1}{4}a_0a_1\mu_\nu^2$			$\frac{1}{4}b_1\mu_\nu^2$

Equation 53 is written in tabular form where the coefficients in the boxes must be multiplied by row and column heads. Values of σ_{nc} and σ_{ns} may be obtained by interpolation from tables 4 and 5 for linearly tapered and twisted blades, where

$$c = c_o(1 + t\, x) \quad \text{from} \quad x = 0.15 \quad \text{to} \quad x = 1 \tag{54}$$

$$\theta_t = \theta_1 x \tag{55}$$

$$\sigma_o = \frac{c_o}{\pi R} \tag{56}$$

and c_o = extended blade-root chord at $r = 0$

$$t = \frac{\text{tip chord}}{c_o} - 1$$

θ_1 = twist in angle of blade zero lift between axis of rotation and tip

In order to use the tabulated values of σ_{nc} and σ_{ns} for blades with linear twist and taper, it is necessary to take the reference blade-pitch angle, A_o, at the extended blade-root chord, c_o, at $r = x = 0$.

The use of the lower limit, $x_1 = 0.15$, in the computations for the blades having linear taper and twist corresponds to present practice and largely eliminates the necessity of making any reverse-flow correction to the blade thrust. The reverse-flow effects are discussed in the following section.

Additional tables, 6 and 7, give the values of σ_{nc} and σ_{ns} for blades having linear taper from $x = 0.20$ to $x = 1$ and helical twist where

$$\theta_t = \tan^{-1}\left(\frac{\tan\theta_T}{x}\right) \qquad (57)$$

and θ_T = design helix angle at $x = 1$

In this case, the reference station for A_0 is taken at the blade tip. The tables for helical twist are included for convertaplane usage since helical twist would appear to be desirable for a reasonable propeller efficiency. An inner limit of $x_1 = 0.20$ was used for the computation of the values of σ_{hc} and σ_{hs} for this case of helical twist in order to minimize the severe root stall likely to occur under some convertaplane flight conditions. It might be pointed out that helical twist would also appear to afford an increase in helicopter-rotor performance over that obtainable with linear twist.

Reverse-Flow Considerations

For normal helicopter and convertaplane flight conditions where there is a downflow through the rotor and ϕ_w is negative over the reverse-flow region, the maximum value of μ_w is limited to relatively low values of the order of 0.30 by tip stall on the retreating blades. Under these conditions the portion of the retreating blade extending inboard from the outer edge of the reverse-flow region at $x = -\mu_w \sin\psi$ where the in-plane component of velocity is zero, to $x = x_1$, where the blade-airfoil section ends, has a negligible thrust loading because the in-plane components of velocity are very small. The present equations take into account the fact that the blade airfoil does not exist inboard of $x = x_1$, for which region the in-plane components of velocity are larger, within the reverse-flow circle, and previous equations erred in assuming the blade airfoil to exist.

For those flight conditions where there is an upflow through the rotor and the tip-stall limitations on μ_N are relaxed, the present equations give the proper direction to the blade-element thrust for those blade elements within the reverse-flow region and inside the radius where $\phi_N \approx 2\theta_N$.

Thus, for all practical purposes, it is not necessary to use reverse-flow corrections when applying the present equations to conventional rotors.

Mean Rotor Thrust

Omitting the coefficients of the second harmonic flapping angle which have a negligible effect on the mean rotor thrust, the value of the mean rotor thrust coefficient obtained from row 1 of equation 53 is

$$\frac{2C_T}{ab} = \left[1 + \tfrac{1}{2}a_1(\gamma - \omega_x) - \tfrac{1}{2}b_1(w + \omega_y)\right] I_{3C} + \tfrac{1}{2}a_0 b_1 \mu_N I_{2C}$$

$$+ \tfrac{1}{2}(a_1\lambda_N + \mu_N)\mu_N I_{1C} - \left[\lambda_N - a_1\mu_N + \tfrac{1}{2}(\gamma - \omega_x)\mu_N\right] I_{2S} \qquad (58)$$

Mean Rotor Air-Rolling Moment

The value of the mean rotor air-rolling moment coefficient, C_{mx}, about the X axis

where $C_{mx} = \dfrac{M_x}{\frac{1}{2}\rho\pi\Omega^2 R^5}$

is found, upon integration, to be obtained by multiplying the second row of equation 53 by $\frac{1}{2}b$ and writing the subscripts of I_{nC} and I_{nS} to one higher order.

Thus,

$$\frac{2C_{mx}}{ab} = \left[2\mu_v + a_1\lambda_v + \frac{3}{4}a_1(\gamma - \omega_x)\mu_v - \frac{1}{4}b_1(w + \omega_y)\mu_v\right] I_{3C}$$

$$+ \frac{1}{4}a_0 b_1 \mu_v^2 I_{2C} + (a_1 - \gamma + \omega_x) I_{4S}$$

$$+ \left(\frac{3}{4}a_1\mu_v - \lambda_v\right)\mu_v I_{2S} \qquad (59)$$

Mean Rotor Air-Pitching Moment

Similarly, the mean rotor air-pitching moment coefficient

$$C_{my} = \frac{M_y}{\frac{1}{2}\rho\pi\Omega^2 R^5}$$

obtained from the third row of equation 53 is

$$\frac{2C_{my}}{ab} = \left[b_1\lambda_v - \frac{1}{4}a_1(w + \omega_y)\mu_v + \frac{1}{4}b_1(\gamma - \omega_x)\mu_v\right] I_{3C}$$

$$+ \frac{1}{4}a_0 a_1 \mu_v^2 I_{2C} + (b_1 + w + \omega_y) I_{4S}$$

$$- a_0\mu_v I_{3S} + \frac{1}{4}b_1\mu_v^2 I_{2S} \qquad (60)$$

Mean Blade-Root Air Moment

The coefficient, C_{mo}, of the blade-root air moment, M_o, is merely the first row of equation 53 with the I factors to one higher subscript. Thus, for $C_{mo} = \frac{M_o}{\frac{1}{2}\rho\pi\Omega^2 R^5}$

$$\frac{C_{mo}}{a} = \left[1 + \tfrac{1}{2}a_1(q - \omega_x) - \tfrac{1}{2}b_1(w + \omega_y)\right] I_{4C} + \tfrac{1}{2}a_o b_1 \mu_w I_{3C}$$

$$+ \tfrac{1}{2}(a_1\lambda_w + \mu_w)\mu_w I_{2C} - \left[\lambda_w - a_1\mu_w + \tfrac{1}{2}(q - \omega_x)\mu_w\right] I_{3S} \quad (61)$$

Equilibrium Values of the Mean Rotor Pitching Moment and Rolling Moment

If an external moment, M_1, be applied to a single rotor with three or more blades about a diameter, axis 1, the differential equations of motion about axis 1 at $\psi = \psi_1$, and axis 2 at $\psi = \psi_1 + 90^\circ$ can be shown by the use of Euler's equations to be

$$\frac{d\omega_1}{dt} + \Omega\omega_2 + \frac{k_1\omega_1}{I_w} = \frac{M_1}{I_w} \quad (62)$$

and $$\frac{d\omega_2}{dt} - \Omega\omega_1 + \frac{k_2\omega_2}{I_w} = 0 \quad (63)$$

where ω_1 and ω_2 are the angular velocities of the tip-path plane about axes 1 and 2, respectively.

$k_1\omega_1$ and $k_2\omega_2$ are the damping moments

I_w is the mass moment of inertia of the rotor about the virtual axis of rotation.

The general solution of equations 62 and 63 is a pair of equations of the form

$$\omega_{1 \text{ or } 2} = \left[A\sin\sqrt{\Omega^2 - \left(\frac{k_1 - k_2}{2I_w}\right)^2}\, t + B\cos\sqrt{\Omega^2 - \left(\frac{k_1 - k_2}{2I_w}\right)^2}\, t\right] e^{-\frac{k_1 + k_2}{2I_w}t} \quad (64)$$

In the actual case, damping of the nutation appears to be very rapid for an articulated rotor. Also, for pilot-controlled motion, $k_2 \approx 0$. For example, for a constant control moment, M_1, $k_2 = 0$ and $k_1 = 2\Omega I_v$ the value for critical damping

$$\omega_1 = \frac{2M_1 t}{I_v} e^{-\Omega t} \tag{65}$$

$$\omega_2 = \frac{M_1}{I_1 \Omega}(1 - e^{-\Omega t}) \tag{66}$$

It can be seen from equations 65 and 66 that the transients decay very rapidly and their effects can be neglected in most problems. Therefore, to a good approximation for a single rotor

$$M_x = I_v \Omega \omega_y + M_{xf} \tag{67}$$

$$M_y = -I_v \Omega \omega_x + M_{yf} \tag{68}$$

where M_{xf} and M_{yf} are any moments transmitted about the X and Y axes from the fuselage to the rotor.

For steady straight and level flight

$$\omega_x = \omega_y = 0 \tag{69}$$

For steady banked turns the value of C_T can be taken proportional to $\sec \theta_x$. Also

$$\omega_x \approx \frac{g \sin \theta_x \tan \theta_x}{V} \tag{70}$$

and

$$\omega_y \approx \frac{g \sin\theta_y \tan\theta_x}{V} \tag{71}$$

where θ_x is the equilibrium lateral-tilt angle of the tip-path plane (approximately equal to equilibrium angle of bank, positive for turns in direction of rotor rotation)

For any curvature of the flight path, the components, ω_x and ω_y, of the aircraft's spatial angular velocity may be calculated and, consequently, the approximate equilibrium values of M_x and M_y can be obtained from equations 67 and 68.

Approximate Solution for Equilibrium Values of the Mean Reference Blade Angle, A_o, the Lateral and Longitudinal Components of the Cyclic Pitch, $-a_1$, and b_1, and the Coning Angle, a_o.

An approximate solution of the set of four non-linear, transcendental equations, 58, 59, 60, and 61, for the four unknowns, A_o, a_1, a_o, and b_1, that is sufficiently accurate for most steady-flight helicopter work and useful as a first trial for steady-flight convertaplane calculations may be obtained as follows: setting the small terms and ω_x, ω_y, and C_{mx} equal to zero and cos A_o = 1 in equations 58 and 59, and eliminating a_1, gives

$$\sin A_o = \frac{\left(\frac{2C_T}{ab} - \sigma_{3s} - \lambda_w\sigma_{2c}\right)\left(\sigma_{4c} + \frac{3}{4}\mu_w^2\sigma_{2c} - \lambda_w\sigma_{3s}\right) + \mu_w^2\sigma_{2c}\left(2\sigma_{3s} + \lambda_w\sigma_{2c}\right)}{\left(\sigma_{3c} + \frac{1}{2}\mu_w^2\sigma_{1c} - \lambda_w\sigma_{2s}\right)\left(\sigma_{4c} + \frac{3}{4}\mu_w^2\sigma_{2c} - \lambda_w\sigma_{3s}\right) - 2\mu_w^2\sigma_{2c}\sigma_{3c}} \tag{72}$$

Then, from equation 59 for $\omega_x = \omega_y = C_{mx} = 0$

$$a_1 = -\frac{2\mu_\nu I_{3C} - \gamma I_{4S} - \lambda_\nu \mu_\nu I_{2S}}{\left(\lambda_\nu + \frac{3}{4}\gamma\mu_\nu\right) I_{3C} + I_{4S} + \frac{3}{4}\mu_\nu^2 I_{2S}} \qquad (73)$$

Let $\bar{a}_o$ be the design coning angle for the general case of semi-rigid blades (i.e. coning angle for zero blade-root bending moment). Let k_{a_o} be the spring constant of the blade for angular deflections of the three-quarter radius point from $\bar{a}_o$. Then setting the summation of moments about the blade root equal to zero and solving for a_o, the coning angle at the three-quarter radius point,

$$a_o \approx \frac{\frac{1}{2}\rho\pi a \Omega^2 R^5 \left[I_{4C} + \frac{1}{2}(a_1\lambda_\nu + \mu_\nu)\mu_\nu I_{2C} - (\lambda_\nu - a_1\mu_\nu) I_{3S}\right] + \bar{a}_o k_{a_o} - M_B \bar{r} g}{I_1 \Omega^2 + k_{a_o}} \qquad (74)$$

where M_B = mass of blade

$\bar{r}$ = radius of blade c.g.

I_1 = mass moment of inertia of blade about flapping hinge (or root)

(Note: If the blades have a flapping hinge at the axis of rotation $\bar{a}_o = k_{a_o} = 0$. If the flapping hinge is located at radius, r_β, from the axis of rotation, $\bar{a}_o = 0$ and $k_{a_o} \approx \frac{r_\beta \bar{r} M_B \Omega^2}{1 - \frac{r_\beta}{0.75R}}$

Then, knowing a_o, it follows from equation 60, that for

$$\omega_x = \omega_y = C_{my} = 0$$

$$b_1 \approx \frac{a_0 \mu_v I_{3S} - \mu_v I_{4S}}{\lambda_v I_{3C} + I_{4S} + \frac{1}{4}\mu_v^2 I_{2S}} \tag{75}$$

For those steady, unaccelerated flight conditions where $\cos A_0 \approx 1$, the above solutions are sufficiently accurate and may be used to calculate the blade loadings and rotor torque, X force, and Y force.

"Exact" Solution for A_0, a_1, and b_1, for Accelerated Flight Conditions and Those Flight Conditions Where $\cos A_0 \neq 1$.

A reasonably rapid and sufficiently accurate solution of the "exact" equilibrium equations given by the first three rows of equation 53 can be obtained by using an approximate value for the coning angle, a_0, such as that given by equation 74 or that following equation 23.

Then for the approximate value of A_0 given by equation 72 and, for example, two other values several degrees successively smaller, the "exact" corresponding values of a_1 and b_1 can be determined by rewriting the equilibrium equations for the rotor pitching and rolling moments in the form

$$A a_1 + B b_1 = P - \frac{2 C_{my}}{a}$$

and

$$C a_1 + D b_1 = R + \frac{2 C_{mx}}{a} \tag{76}$$

where

$$A = \frac{1}{4}(w + \omega_y)\mu_v I_{3C} - \frac{1}{4} a_0 \mu_v^2 I_{2C} \tag{77}$$

$$B = -\lambda_v I_{3C} - \frac{1}{4}(y - \omega_x)\mu_v I_{3C} - I_{4S} - \frac{1}{4}\mu_v^2 I_{2S} \tag{78}$$

$$C = \lambda_v I_{3C} + \frac{3}{4}(y - \omega_x)\mu_v I_{3C} + I_{4S} + \frac{3}{4}\mu_v^2 I_{2S} \tag{79}$$

$$D = -\frac{1}{4}(w + \omega_y)\mu_v I_{3C} + \frac{1}{4} a_o \mu_v^2 I_{2C} \tag{80}$$

$$P = (w + \omega_y) I_{4S} - a_o \mu_v I_{3S} \tag{81}$$

$$R = -2\mu_v I_{3C} + (y - \omega_x) I_{4S} + \lambda_v \mu_v I_{2S} \tag{82}$$

Then

$$a_1 = \frac{\begin{vmatrix} \left(P - \frac{2C_{my}}{a}\right) & B \\ \left(R + \frac{2C_{mx}}{a}\right) & D \end{vmatrix}}{\begin{vmatrix} A & B \\ C & D \end{vmatrix}} \tag{83}$$

and

$$b_1 = \frac{\begin{vmatrix} A & \left(P - \frac{2C_{my}}{a}\right) \\ C & \left(R + \frac{2C_{mx}}{a}\right) \end{vmatrix}}{\begin{vmatrix} A & B \\ C & D \end{vmatrix}} \tag{84}$$

Having computed the values of a_1 and b_1 for each of the assumed values of A_o, the corresponding values of C_T may be found from the equation for the thrust equilibrium where

$$\frac{2C_T}{a} = I_{3C} + \frac{1}{2}\mu_\nu^2 I_{1C} - \lambda_\nu I_{2S} - \frac{1}{2}(\eta_y - \omega_x)\mu_\nu I_{2S}$$

$$+\left[\frac{1}{2}(\eta_y - \omega_x) I_{3C} + \frac{1}{2}\lambda_\nu \mu_\nu I_{1C} + \mu_\nu I_{2S}\right] a_1$$

$$+\left[\frac{1}{2} a_0 \mu_\nu I_{2C} - \frac{1}{2}(w + \omega_y) I_{3C}\right] b_1 \qquad (85)$$

Then plotting the values of $\frac{2C_T}{a}$, a_1, and b_1, versus the trial values of A_0, the "exact" value of A_0, and thus a_1 and b_1, may be obtained from the plot at the design or desired value of C_T.

In-Plane Component of Force, F_{xy}, on a Blade at Azimuth Angle, ψ.

The in-plane component in the direction of rotation, F_{xy}, on a blade at azimuth angle, ψ, is from equations 37 and 40

$$F_{xy} = \frac{1}{2}\rho a \int_{r_1}^{R} c(U\sin\phi_\nu)\left[\sin\theta_\nu(U\cos\phi_\nu) + \cos\theta_\nu(U\sin\phi_\nu)\right] dr$$

$$-\frac{1}{2}\rho \int_{r_1}^{R} c(U\cos\phi_\nu)\left\{\varepsilon_0 U + \varepsilon_1\left[\sin\theta_\nu(U\cos\phi_\nu) + \cos\theta_\nu(U\sin\phi_\nu)\right]\right.$$

$$\left. + \varepsilon_2\left[\cos\theta_\nu(U\cos\phi_\nu) - \sin\theta_\nu(U\sin\phi_\nu)\right]\right\} \qquad (86)$$

where $c_{d_0} = \varepsilon_0 + \varepsilon_1 \sin\alpha_r + \varepsilon_2 \cos\alpha_r$

Then, by the following operations: substituting the previously evaluated expressions for $U\cos\phi_\nu$, $U\sin\phi_\nu$, $\sin\theta_\nu$, and $\cos\theta_\nu$ given by equations 42, 43, 47, and 48; neglecting the effects of second harmonic

flapping; expanding the expression

$$\frac{U}{U\cos\phi_w} = \sqrt{1+\left(\frac{U\sin\phi_w}{U\cos\phi_w}\right)^2}$$

by the binomial theorem and dropping third and higher terms, the expression for the constant and first harmonic terms becomes

$$C_{xy} = \frac{F_{xy}}{\frac{1}{2}\rho\pi\Omega^2R^4} = (\Delta C_{xy})_a - (\Delta C_{xy})_{\epsilon_0} - (\Delta C_{xy})_{\epsilon_1} - (\Delta C_{xy})_{\epsilon_2} \qquad (87)$$

where $\frac{(a C_{xy})_a}{d} =$

	I_{3C}	I_{2C}	I_{1C}	I_{3S}	I_{2S}	I_{1S}
1		$\lambda_\nu + \frac{1}{2}(\eta - \omega_x)\mu_\nu$ $+ a_1(\eta - \omega_x)\lambda_\nu$ $- b_1(\nu + \omega_y)\lambda_\nu$	$a_0 b_1 \lambda_\nu \mu_\nu$	$\frac{1}{2} a_1 (\eta - \omega_x)$ $- \frac{1}{2} b_1 (\nu + \omega_y)$ $- \frac{1}{2}(\eta - \omega_x)^2$ $- \frac{1}{2}(\nu + \omega_y)^2$	$\frac{1}{2} a_0 b_1 \mu_\nu$ $+ a_0(\nu + \omega_y)\mu_\nu$	$\frac{1}{2} a_1 \lambda_\nu \mu_\nu$ $- \lambda_\nu^2 - \frac{1}{2} a_0^2 \mu_\nu^2$
$\sin\psi$	$\eta - \omega_x$ $+ \frac{3}{4} a_1 (\eta - \omega_x)^2$ $- \frac{1}{2} b_1 (\eta - \omega_x)(\nu + \omega_y)$ $+ \frac{1}{4} a_1 (\nu + \omega_y)^2$	$\frac{1}{2} a_0 b_1 (\eta - \omega_x)\mu_\nu$ $- \frac{1}{2} a_0 a_1 (\nu + \omega_y)\mu_\nu$	$(a_1 \lambda_\nu + \mu_\nu)\lambda_\nu$ $+ \frac{1}{4} a_0^2 a_1 \mu_\nu^2$		$(a_1 - 2\eta + 2\omega_x)\lambda_\nu$ $+ \frac{3}{4} a_1 (\eta - \omega_x)\mu_\nu$ $- \frac{1}{4} b_1 (\nu + \omega_y)\mu_\nu$	$\frac{1}{4} a_0 b_1 \mu_\nu^2$
$\cos\psi$	$\nu + \omega_y$ $- \frac{1}{4} b_1 (\eta - \omega_x)^2$ $+ \frac{1}{2} a_1 (\eta - \omega_x)(\nu + \omega_y)$ $- \frac{3}{4} b_1 (\nu + \omega_y)^2$	$- a_0 \mu_\nu$ $- \frac{1}{2} a_0 a_1 (\eta - \omega_x)\mu_\nu$ $+ \frac{3}{2} a_0 b_1 (\nu + \omega_y)\mu_\nu$	$- b_1 \lambda_\nu^2$ $- \frac{3}{4} a_0^2 b_1 \mu_\nu^2$		$\frac{1}{4} a_1 (\nu + \omega_y)\mu_\nu$ $- b_1 \lambda_\nu$ $- \frac{1}{4} b_1 (\eta - \omega_x)\mu_\nu$ $- 2(\nu + \omega_y)\lambda_\nu$	$- \frac{1}{4} a_0 a_1 \mu_\nu^2$ $+ 2 a_0 \lambda_\nu \mu_\nu$

and $\dfrac{(\Delta C_{xy})_{\varepsilon_0}}{\varepsilon_0} =$

	σ_3	σ_2	σ_1
1	$1 + \frac{1}{4}(w + \omega_y)^2 + \frac{1}{4}(y - \omega_x)^2$	$-\frac{1}{2} a_0 (w + \omega_y) \mu_\nu$	$\frac{1}{2}\left[\lambda_\nu^2 + (1 + \frac{1}{2} a_0^2)\mu_\nu^2\right]$
Sin ψ		$(y - \omega_x)\lambda_\nu + 2\mu_\nu$	
Cos ψ		$(w + \omega_y)\lambda_\nu$	$-a_0 \lambda_\nu \mu_\nu$

and $\frac{(\Delta C_{xy})\varepsilon_1}{\varepsilon_1} =$

	I_{3C}	I_{2C}	I_{1C}	I_{3S}	I_{2S}	I_{1S}
1	1 $+\frac{1}{2}a_1(\gamma-\omega_x)$ $-\frac{1}{2}b_1(w+\omega_y)$	$\frac{1}{2}a_0 b_1 \mu_w$	$\frac{1}{2}(a_1\lambda_w+\mu_w)\mu_w$		$a_1\mu_w-\lambda_w$ $-\frac{1}{2}(\gamma-\omega_x)\mu_w$	
$\sin\psi$		$2\mu_w+a_1\lambda_w$ $+\frac{3}{4}a_1(\gamma-\omega_x)\mu_w$ $-\frac{1}{4}b_1(w+\omega_y)\mu_w$	$\frac{1}{4}a_0 b_1 \mu_w^2$	$a-(\gamma-\omega_x)$		$(\frac{3}{4}a_1\mu_w-\lambda_w)\mu_w$
$\cos\psi$		$\frac{1}{4}a_1(w+\omega_y)\mu_w$ $-\frac{1}{4}b_1(\gamma-\omega_x)\mu_w$ $-b_1\lambda_w$	$-\frac{1}{4}a_0 a_1 \mu_w^2$	$-b_1-(w+\omega_y)$	$a_0\mu_w$	$-\frac{1}{4}b_1\mu_w^2$

and $\frac{(\Delta C_{xy})_{\varepsilon_2}}{\varepsilon_2} =$

Equation 88

	I_{3C}	I_{2C}	I_{1C}	I_{3S}	I_{2S}	I_{1S}
1		$a_1\mu_\nu - \lambda_\nu$ $-\frac{1}{2}(\gamma-\omega_x)\mu_\nu$		-1 $-\frac{1}{2}a_1(\gamma-\omega_x)$ $+\frac{1}{2}b_1(\omega+\omega_y)$	$-\frac{1}{2}a_0 b_1 \mu_\nu$	$-\frac{1}{2}(a_1\lambda_\nu+\mu_\nu)\mu_\nu$
	a_1 $-(\gamma-\omega_x)$		$(\frac{3}{4}a_1\mu_\nu-\lambda_\nu)\mu_\nu$		$-2\mu_\nu - a_1\lambda_\nu$ $-\frac{3}{4}a_1(\gamma-\omega_x)\mu_\nu$ $+\frac{1}{4}b_1(\omega+\omega_y)\mu_\nu$	$-\frac{1}{4}a_0 b_1 \mu_\nu^2$
	$-b_1$ $-(\omega+\omega_y)$	$a_0\mu_\nu$	$\frac{1}{2}(a_0-\frac{1}{2}b_1)\mu_\nu^2$		$-\frac{1}{4}a_1(\omega+\omega_y)\mu_\nu$ $+\frac{1}{4}b_1(\gamma-\omega_x)\mu_\nu$ $+b_1\lambda_\nu$	$\frac{1}{4}a_0 a_1 \mu_\nu^2$

As previously mentioned, it is preferable to use the two-term series approximation for c_{d_o} for those convertaplane flight conditions where $|\lambda_w|$ becomes large (i.e. $|\lambda_w| > 0.10$). For these cases the terms involving ε_o in the preceding equation and following equations may be disregarded. The values of ε_1 and ε_2 will of course be different for the two-term and three-term approximations for c_{d_o}, as pointed out in the discussion on the use of airfoil data.

Rotor Torque

The value of the rotor torque coefficient, C_Q, is

$$\frac{2C_Q}{b} = -\text{(constant terms of } C_{xy} \text{ with subscripts, } n \text{ on } \sigma_n, I_{nc}, \text{ and } I_{ns} \text{ increased to n + 1)} \qquad (89)$$

For steady state calculations where $\omega_x = \omega_y = 0$, an approximate solution that is sufficiently accurate for most purposes may be obtained by neglecting small terms. Then

$$\begin{aligned}\frac{2C_Q}{b} \approx -a\left[\lambda_w I_{3c} + \tfrac{1}{2}a_o(b_1+2w)\mu_w I_{3s} + (\tfrac{1}{2}a_1\mu_w - \lambda_w)\lambda_w I_{2s}\right] \\ + \varepsilon_o\left[(1+\tfrac{1}{4}w^2)\sigma_4 - \tfrac{1}{2}a_o w\mu_w\sigma_3 + \tfrac{1}{2}(\lambda_w^2+\mu_w^2)\sigma_2\right] \\ + \varepsilon_1\left[I_{4c} + \tfrac{1}{2}a_o b_1\mu_w I_{3c} + \tfrac{1}{2}(\mu_w + a_1\lambda_w)\mu_w I_{2c} + (a_1\mu_w - \lambda_w)I_{3s}\right] \\ + \varepsilon_2\left[(a_1\mu_w - \lambda_w)I_{3c} - (1-\tfrac{1}{2}b_1 w)I_{4s} - \tfrac{1}{2}a_o b_1\mu_w I_{3s}\right. \\ \left. - \tfrac{1}{2}(a_1\lambda_w + \mu_w)\mu_w I_{2s}\right]\end{aligned} \qquad (90)$$

Rotor X-Force

The value of the rotor X-force coefficient, C_x , is

$$\frac{2C_x}{b} = - \text{(sine terms of } C_{xy}) \tag{91}$$

For steady-state solutions the expression may be simplified to

$$\begin{aligned}\frac{2C_x}{b} \approx -a\Big[&\gamma I_{3C} + (a_1\lambda_w + \mu_w)\lambda_w I_{1C} \\ &+ (a_1\lambda_w - 2\gamma\lambda_w + \tfrac{3}{4}a_1\gamma\mu_w - \tfrac{1}{4}b_1\mu_w)I_{2S}\Big] \\ &+ \varepsilon_0\Big[(\gamma\lambda_w - 2\mu_w)\sigma_2\Big] \\ &+ \varepsilon_1\Big[(a_1\lambda_w + 2\mu_w)I_{2C} + (a_1 - \gamma)I_{3S} + (\tfrac{3}{4}a_1\mu_w - \lambda_w)\mu_w I_{1S}\Big] \\ &+ \varepsilon_2\Big[(a_1 - \gamma)I_{3C} + (\tfrac{3}{4}a_1\mu_w - \lambda_w)\mu_w I_{1C} - (2\mu_w + a_1\lambda_w)I_{2S}\Big]\end{aligned} \tag{92}$$

Rotor Y-Force

Similarly, the value of the rotor Y-force coefficient is

$$\frac{2C_y}{b} = \text{(cosine terms of } C_{xy}) \tag{93}$$

and for steady-state solutions this expression may be simplified for most purposes to

$$\begin{aligned}\frac{2C_y}{b} \approx a\Big[&\mu_w I_{3C} - a_0\mu_w I_{2C} - b_1\lambda_w^2 I_{1C} \\ &+ (\tfrac{1}{4}a_1\omega\mu_w - \tfrac{1}{4}b_1\gamma\mu_w - b_1\lambda_w - 2\omega\lambda_w)I_{2S} \\ &+ (2a_0\lambda_w + \tfrac{1}{4}a_0a_1\mu_w)\mu_w I_{1S}\Big]\end{aligned} \tag{94}$$

Second Harmonic Flapping

Again letting k_{a_o} be the spring constant relating the blade-root bending moment in foot pounds to the angular deflection in radians of the three-quarter radius point of the blades from the unstressed position, it follows that the magnitude of the cosine component of the second harmonic of the blade-flapping angle is

$$a_2 \approx \frac{J + KL}{1 - KM} \tag{95}$$

Similarly the magnitude of the sine component is

$$b_2 \approx \frac{L + JM}{1 - KM} \tag{96}$$

where J = (terms not involving b_2 in the cos 2ψ row of thrust equation 53 with the I factors changed to one higher subscript) $\left(\frac{\frac{1}{2}\rho\pi\Omega^2R^5a}{3I_1\Omega^2 + k_{a_o}}\right)$

K = (coefficients of b_2 in the cos 2ψ row of thrust equation 53 with the I factors changed to one higher subscript) $\times$ $\left(\frac{\frac{1}{2}\rho\pi\Omega^2R^5a}{3I_1\Omega^2 + k_{a_o}}\right)$

L = (terms not involving a_2 in the sine 2ψ row of thrust equation 53 with the I factors changed to one higher subscript) $\left(\frac{\frac{1}{2}\rho\pi\Omega^2R^5a}{3I_1\Omega^2 + k_{a_o}}\right)$

M = (coefficients of a_2 in the sine 2ψ row of thrust equation 53 with the I factors changed to one higher subscript) $\times$ $\left(\frac{\frac{1}{2}\rho\pi\Omega^2R^5a}{3I_1\Omega^2 + k_{a_o}}\right)$

For steady-state flight conditions where = = 0 the expressions for the factors, J, K, L, and M may be simplified to

$$J \approx \frac{\frac{1}{2}\rho \pi a \Omega^2 R^5}{3I_1\Omega^2 + k_{a_0}} \left[-\frac{1}{2}(a_1 \lambda_w + \mu_w)\mu_w I_{2C} \right.$$

$$\left. -(a_1 - \tfrac{1}{2}\gamma)\mu_w I_{3S} \right] \tag{97}$$

$$K \approx \frac{\frac{1}{2}\rho \pi a \Omega^2 R^5}{3I_1\Omega^2 + k_{a_0}} \left[-2I_{4S} \right] \tag{98}$$

$$L \approx \frac{\frac{1}{2}\rho \pi a \Omega^2 R^5}{3I_1\Omega^2 + k_{a_0}} \left[-\frac{1}{2} b_1 \lambda_w \mu_w I_{2C} \right.$$

$$\left. -(b_1 + \tfrac{1}{2}\mu^2)\mu_w I_{3S} + \tfrac{1}{2} a_0 \mu_w^2 I_{2S} \right] \tag{99}$$

$$M \approx \frac{\frac{1}{2}\rho \pi a \Omega^2 R^5}{3I_1\Omega^2 + k_{a_0}} \left[2I_{4S} \right] \tag{100}$$

and I_1 = mass moment of inertia of blade about flapping hinge.

It may be noted that k_{a_0} = 0 for blades having a flapping hinge at the axis of rotation. If the flapping hinge is located at radius, r_β, then

$$k_{a_0} \approx \frac{r_\beta \bar{F} M_B \Omega^2}{1 - \frac{r_\beta}{0.75R}}$$

Amplitude of the Constant and First Harmonic Components of the Lag Angles In Unaccelerated Flight.

For an articulated rotor having lag hinges normal to the plane of rotation and located at a small radius, e , the equilibrium blade lag angle, E_o , is

$$E_o \approx \frac{\frac{1}{2}\rho\pi R^5}{M_\zeta e\left(1-\frac{e}{0.7R}\right)}\left[-\frac{2C_Q}{b}\quad \text{from equation 90}\right] \tag{101}$$

where M_ζ = mass moment of blade about lag hinge.

Similarly the coefficients of the cosine and sine components of the lag angle are

$$E_1 \approx \frac{\frac{1}{2}\rho\pi R^5 E_\zeta - 2a_o b_{1S} I_\zeta}{M_\zeta e - I_\zeta} \tag{102}$$

and

$$F_1 \approx \frac{\frac{1}{2}\rho\pi R^5 F_\zeta + 2a_o a_{1S} I_\zeta}{M_\zeta e - I_\zeta} \tag{103}$$

where a_{1S} and b_{1S} are the $\cos\psi$ and $\sin\psi$ components of the angle between the tip-path plane and the hub plane.

For unaccelerated flight the values of a_{1S} and b_{1S} are approximately

$$a_{1S} \approx \alpha_w - \alpha_f \tag{104}$$

$$b_{1S} \approx \theta_{\chi f} - \theta_\chi \tag{105}$$

where $\theta_{\chi f}$ = equilibrium lateral tilt of fuselage.

Also I_ζ = mass moment of inertia of a blade about the lag hinge

E_ζ = coefficient of cosine ψ in equation 88 for C_{xy} with subscripts of I factors changed from n to n + 1

or

$$E_\zeta \approx a\left[w I_{4c} - a_0 \mu_w I_{3c} - (6_1 + 2w)\lambda_w I_{3s} + 2 a_0 \lambda_w \mu_w I_{2s}\right] \tag{106}$$

F_ζ = coefficient of sin ψ in equation 88 for C_{xy} with subscripts of I factors changed fro, n to n + 1

or

$$F_\zeta \approx a\left[\gamma I_{4c} + \lambda_w \mu_w I_{2c} + (a_1 - 2\gamma)\lambda_w I_{3s}\right]$$

$$-\varepsilon_0\left[(\gamma\lambda_w + 2\mu_w)\sigma_3\right]$$

$$-\varepsilon_1\left[2\mu_w I_{3c} + a_1 I_{4s} + \left(\tfrac{3}{4} a_1 \mu_w - \lambda_w\right)\mu_w I_{2s}\right]$$

$$-\varepsilon_2\left[(a_1 - \gamma) I_{4c} + \left(\tfrac{3}{4} a_1 \mu_w - \lambda_w\right)\mu_w I_{2c} - 2\mu_w I_{3s}\right] \tag{107}$$

Thrust Unbalance

Two-bladed rotor. - The second harmonic variation in C_T for a two-bladed rotor is

$$\frac{\Delta C_T}{a} = 4th + 5th \text{ rows of equation } 53 \tag{108}$$

For $\omega_x = \omega_y = 0$ and steady state conditions, the equation for the amplitude may be simplified to

$$\frac{\Delta C_T}{a} \approx \left\{\left[2a_2 I_{3S} - (b_1 + \tfrac{1}{2}w)\mu_N I_{2S} + \tfrac{1}{2} a_0 \mu_N^2 I_{1S}\right]^2 + \left[2b_2 I_{3S} + a_1 \mu_N I_{2S}\right]^2\right\}^{\frac{1}{2}} \tag{109}$$

Three-bladed rotor. - The third harmonic variation in C_T for a three-bladed rotor is approximately

$$\frac{2\Delta C_T}{3a} \approx 6th + 7th \text{ rows of equation } 53 \tag{110}$$

or for $\omega_x = \omega_y = 0$ the amplitude is approximately

$$\frac{2\Delta C_T}{3a} \approx -\frac{1}{4}\left(a_1^2 + b_1^2\right)^{\frac{1}{2}} \mu_N^2 I_{1S} \tag{111}$$

An Independence-of-Blade-Element Analysis for Hovering, Vertical Ascent, and the Convertaplane Propeller Condition.

The use of the relation $C_l = a \sin \alpha$ permits a considerable simplification of the equations resulting from the assumption of the independence of blade elements. As the "exact" propeller solutions of Betz, Goldstein, and Theodorsen are not applicable to a lifting rotor at zero or small advance ratios, a simple independence of blade element analysis may be useful.

From momentum considerations the thrust, dT, on an annulus of the rotor disk, $2\pi r dr$, is related to the induced velocity, V_i, at the rotor element by the expression

$$\frac{dT}{4\pi\rho r\,dr} = V_i\left(V_i + V\sin\alpha_r\right) \tag{112}$$

but $$V_i + V\sin\alpha_r = U\sin\phi_r \tag{113}$$

Thus $$\frac{dT}{4\pi\rho r\,dr} = \left(U\sin\phi_r\right)\left(U\sin\phi_r - V\sin\alpha_r\right) \tag{114}$$

The thrust of the annulus is also equal to the thrust acting on the portions of the blades within the annulus which is

$$dT = \tfrac{1}{2}\rho b U^2 c\, c_\ell \cos\phi_r\, dr \tag{115}$$

where $$c_\ell = a\sin\alpha_r = a\left(\sin\theta_r\cos\phi_r + \cos\theta_r\sin\phi_r\right) \tag{116}$$

Thus $$dT = \tfrac{1}{2}\rho ab\left(U\cos\phi_r\right)\left[\sin\theta_r\left(U\cos\phi_r + \cos\theta_r\left(U\sin\phi_r\right)\right]\right. c\,dr \tag{117}$$

Substituting the above values of d T in equation 114 and solving for U sin ϕ_r

$$\frac{U\sin\phi_r}{\Omega R} = \left(\frac{\nu_a}{2} + \frac{ab\sigma_r}{16}\cos\theta_r\right) - \sqrt{\left(\frac{\nu_a}{2} + \frac{ab\sigma_r}{16}\cos\theta_r\right)^2 + \frac{ab\sigma_r}{8}\chi\sin\theta_r} \tag{118}$$

where

$$\nu_a = \frac{V \sin \alpha_v}{\Omega R} \tag{119}$$

$$\sigma_r = \frac{c}{\pi R} \tag{120}$$

Then from equation 117

$$\frac{2 C_T}{a b} = \int_{x_1}^{1} \left[x \sin \theta_v + \left(\frac{U \sin \phi_v}{\Omega R} \right) \cos \theta_v \right] \sigma_r x \, dx \tag{121}$$

where the value of $\frac{U \sin \phi_v}{\Omega R}$ at x is given by equation 118.

Similarly from blade-element considerations

$$\frac{2 C_Q}{b} = -a \int_{x_1}^{1} \left(\frac{U \sin \phi_v}{\Omega R} \right) \left[x \sin \theta_v + \left(\frac{U \sin \phi_v}{\Omega R} \right) \cos \theta_v \right] \sigma_r x \, dx$$

$$+ \frac{c_{do}}{\sin \alpha_r} \int_{x_1}^{1} \left[x \sin \theta_v + \left(\frac{U \sin \phi_v}{\Omega R} \right) \cos \theta_v \right] \sigma_r x^2 \, dx \tag{122}$$

where the value of $\frac{c_{do}}{\sin \alpha_r}$ is obtained from a plot of $\frac{c_{do}}{\sin \alpha_r}$ versus α_r for the blade airfoil at

$$\alpha_r = \theta_v + \tan^{-1} \left[\frac{1}{x} \left(\frac{U \sin \phi_v}{\Omega R} \right) \right] \tag{123}$$

If it is necessary to take into account the rotation of the slipstream for large rates of vertical ascent or the propeller condition, this may be accomplished to a first approximation by using an effective Ω, Ω_e, in every case where

$$\Omega_e = \Omega \left(1 - \frac{1}{4} C_T \right) \tag{124}$$

The geometry of the above equations is exact and they are convenient for graphical or numerical integration on account of the repetition of factors.

Neglecting the induced radial and tangential velocity components, the optimum blade-angle distribution for minimum induced power and a given blade-chord distribution and nondimensional axial-flight path velocity, ν_a, may be obtained by setting $\frac{U \sin \phi_r}{\Omega R}$ equal to the constant value λ_r, giving

$$\sin \theta_r = \frac{\lambda_r (\lambda_r - \nu_a) \chi}{k(\lambda_r^2 + \chi^2)} \left\{ 1 + \sqrt{1 + \frac{(\lambda_r^2 + \chi^2)[k^2 - (\lambda_r - \nu_a)^2]}{(\lambda_r - \nu_a)^2 \chi^2}} \right\} \tag{125}$$

where $$k = \frac{a b \sigma_r}{8} \tag{126}$$

and $$\lambda_r = \frac{\nu_a}{2} - \sqrt{\left(\frac{\nu_a}{2}\right)^2 + \frac{1}{2} C_T} \tag{127}$$

The optimum chord distribution for a given desired constant value of c_l along the blade and the same restrictions is

$$\sigma_r = \frac{8 \lambda_r (\lambda_r - \nu_a)}{b c_l \sqrt{\lambda_r^2 + \chi^2}} \tag{128}$$

For this optimum chord distribution, the optimum distribution of θ_r reduces to

$$\sin \theta_r = \frac{\chi c_l}{a \sqrt{\lambda_r^2 + \chi^2}} \left[1 + \sqrt{1 + \frac{a^2 \lambda_r^2 - c_l^2 (\lambda_r^2 + \chi^2)}{c_l^2 \chi^2}} \right] \tag{129}$$

For calculations where the flight-path velocity and equilibrium value of C_T are known or can be estimated, the following procedure may be followed:

1. Calculate and plot the radial distribution of σ_τ

2. Calculate the effective value of C_T and ν_a where

$$C_{Te} = C_T\left(\frac{\Omega}{\Omega_e}\right)^2$$

$$\nu_{ae} = \nu_a\left(\frac{\Omega}{\Omega_e}\right)$$

3. Calculate the approximate value of A_o from equation 72 which for these flight conditions reduces to

$$\sin A_o \approx \frac{\left(\frac{2\,C_{Te}}{ab} - \sigma_{3s} - \lambda_\nu \sigma_{2c}\right)\left(\sigma_{4c} - \lambda_\nu \sigma_{3s}\right)}{\left(\sigma_{3c} - \lambda_\nu \sigma_{2s}\right)\left(\sigma_{4c} - \lambda_\nu \sigma_{3s}\right)}$$

4. Calculate and plot the radial distribution of $\theta_\nu = A_o + \theta_t$ for the value of A_o obtained under Item 3 and two lower values at increments of several degrees.

5. Calculate and plot the radial distribution of $\frac{U \sin \phi_\nu}{\Omega_e R}$ for the above distribution of θ_ν from equation 118 using $\Omega = \Omega_e$ throughout.

6. Calculate and plot the radial distribution of the integrand of equation 121 for the three values of A_o and graphically or numerically integrate for the values of $\frac{2\,C_{Te}}{ab}$ corresponding to the three values of A_o.

7. Obtain the correct value of A_o from a plot of C_{T_e} versus A_o.

8. Calculate and plot the radial distribution of the integrand of equation 122 for the three values of A_o and graphically or

numerically integrate for the values of $\frac{2C_{Qe}}{b}$ corresponding to the three values of A_o.

9. Obtain the equilibrium value of C_{Q_e} at the equilibrium value of A_o from a plot of C_{Q_e} versus A_o.

10. Calculate the equilibrium value of $C_Q = C_{Q_e}\left(\frac{\Omega_e}{\Omega}\right)^2$

Comparison of Experimental and Calculated Values of the Parameters

Table 8 shows a comparison of the experimental data of reference 1 for those runs where $C_T \approx 0.00545$ with the values calculated by the approximate blade-element equations of this report. The blade-element lift-curve slope was taken as $a = 6.5$ from the experimental results of reference 6. The values of ε_o, ε_1, and ε_2 were evaluated for the points $c_{d_o} = 0.0095$, 0.0105, and 0.0140, at $\alpha = 0$, 4, and 8°, respectively, from figure 19 of reference 6.

The "exact" solutions for the various parameters differ from the tabulated approximate solutions by a negligible amount for these helicopter flight conditions.

The values of the parameters from reference 1 calculated for $a = 5.75$ by the previous equations, which are based on the use of an effective solidity and the approximations that θ and ϕ are small angles, are also included in table 8 although the results are not strictly comparable because of the difference in assumed lift-curve slope and profile-drag parameters.

A consideration of the results presented in tables 2 and 8 would indicate that much of the remaining discrepancy between experimental and calculated blade angles and torque coefficients may be due to the neglect,

in the present calculations, of the effects of the rotor induced velocity on the lift and drag of the fuselage.

Also it will be seen from the results of run 2 that the present equations considerably underestimate the power required for those flight conditions where the tip stall on the retreating blades is severe.

If the experimental results of run 7 be assumed correct, it would also appear that the present elementary vortex theory overestimates the magnitude of the mean induced velocity for low speed forward flight, though this seems unlikely.

The present calculated values of the coning and lag angles are slightly too large since standard sea-level air density was used in the calculations in the absence of the experimental values.

It may be noted that the longitudinal component of the angle, $\tan^{-1}\left(\frac{C_x}{2C_T}\right)$, between the rotor resultant force and the thrust component normal to the tip-path plane is very small for all these helicopter flight conditions and that the direction of the resultant is inclined forward for those flight conditions where there is a net downflow through the rotor. The inclinations of the tip-path plane to the horizontal, θ_x and θ_y, are also small angles and consequently for many unaccelerated-flight helicopter calculations the rotor resultant force can be assumed to be perpendicular to the tip-path plane and the thrust equal to the gross weight without introducing serious errors.

CONCLUDING REMARKS

Simple relations for C_Q, C_x, and C_y, derived upon the assumption of a triangular distribution of blade-element circulation along the radius and a sinusoidal variation with azimuth angle in conjunction with a linear variation of profile drag with lift, would appear to be useful for helicopter and convertaplane performance estimation and the determination of the equilibrium angle of attack and lateral tilt of the tip-path plane.

The blade-element equations, based upon the relation that $c_\ell = a \sin \alpha_r = a (\sin \theta_w \cos \phi_w + \cos \theta_w \sin \phi_w)$, and the σ_{hc} and σ_{hs} functions of the blade-chord and blade-twist distribution, afford a reasonably exact and concise treatment of the geometry, and should be useful for convertaplane as well as helicopter calculations provided that there are no large areas of the rotor outside the reverse-flow region where the blade elements are stalled.

The use of the empirical relation, $c_{d_o} = \varepsilon_o + \varepsilon_1 \sin \alpha_r + \varepsilon_2 \cos \alpha_r$, rather than the usual expression that $c_{d_o} = \delta_o + \delta_1 \alpha_r + \delta_2 \alpha_r^2$ considerably simplifies the equations for the in-plane forces and moments and presents a sufficiently exact solution of the geometry for helicopter calculations.

For convertaplane calculations, the approximation that $c_{d_o} = \varepsilon_1 \sin \alpha_r + \varepsilon_2 \cos \alpha_r$ allows an "exact" treatment of the geometry and should be a sufficiently accurate expression for c_{d_o} at the larger advance ratios where the effects of the profile drag become of less relative importance.

The larger sources of the remaining errors in the blade-element analysis probably have the following order of importance for contemporary helicopters:

1. The neglect of the effects of blade-element stall implied in the relation that $c_\ell = a \sin \alpha_r$.
2. The neglect of the effects of blade flexibility.
3. The neglect of the radial variation in the normal component of the induced velocity.
4. The neglect of the effects of compressibility on the tip sections of the advancing blade.

Although Item one above might be eliminated by writing the blade-element lift coefficient as an odd Fourier series in the blade-element angle of attack, this results in great complexities and difficulties with the integrations and the results would probably not be useful. Similar difficulties arise in attempting to write the blade-element profile drag as an even Fourier series in the angle of attack.

The error involved in the neglect of blade deflections would appear to depend to a large extent on the individual design and thus be intractable in a general analysis.

The inclusion of a term in the equation for $\frac{U \sin \phi_w}{\Omega R}$ to account for a radial variation of the induced velocity would be feasible provided that the relation for the necessary constant could be derived from the vortex theory. A reasonable approach might be to assume a triangular distribution of circulation along the blade radius.

It would be very difficult to include the effects of compressibility on the advancing blade tip sections in present blade-element analysis on

account of the complexities that arise in defining the boundaries of the affected rotor area.

Thus, of the larger remaining sources of error in present blade-element theory, only that arising from the neglect of the radial variation in the induced velocity would appear to be amenable to correction.

REFERENCES

1. Myers, Garry C., Jr.: Flight Measurements of Helicopter Blade Motion with a Comparison Between Theoretical and Experimental Results. T.N. No. 1266, NACA, April 1947.

2. Meijer Drees, Jr.: A Theory of Airflow Through Rotors and Its Application to Some Helicopter Problems. The Journal of the Helicopter Association of Great Britain, Vol. 3, No. 2, July-August-September 1949, pp. 79-104.

3. Castles, Walter, Jr., and Gray, Robin B.: Wind Tunnel Tests On Four Model Rotors In Vertical Descent. Unpublished. (NACA Contract NAw 5527)

4. Glauert, H.: Airplane Propellers. The Blade Element Theory. Vol. IV, div. L, sec. 9, ch. V of Aerodynamic Theory, W. F. Durand, ed., Julius Springer (Berlin), 1935.

5. Young, A. D., and Winterbottom, N. E.: Note on the Effect of Compressibility on the Profile Drag of Airfoils at Subsonic Mach Numbers in the Absence of Shock Waves. R and M 2400, British A.R.C., 1950.

6. Tetervin, Neal: Airfoil Section Data From Tests Of 10 Practical-Construction Sections Of Helicopter Rotor Blades Submitted By The Sikorsky Aircraft Division, United Aircraft Corporation. Wartime Rep. No. L-643, NACA, Sept. 1944.

7. Gustafson, F. B., and Gersow, Alfred: Flight Tests of the Sikorsky HNS-1 (Army YR-4B) Helicopter. II - Hovering and Vertical-Flight Performance With the Original and an Alternate Set of Main-Rotor Blades Including a Comparison With Hovering Performance Theory. Wartime Rep. No. L-596, NACA, April 1945.

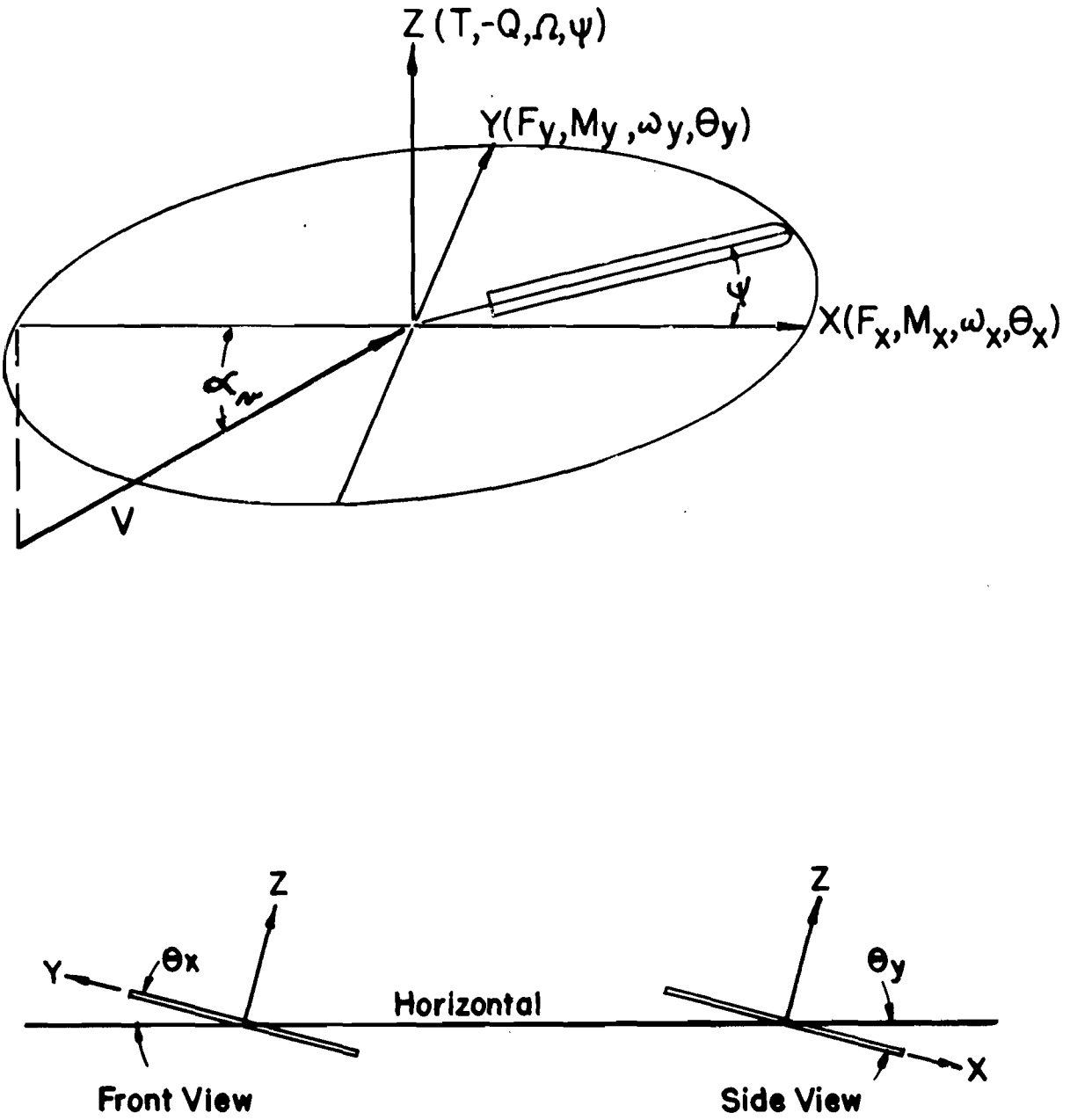

Figure I Tip-Path Plane or Axes of Virtual Rotation

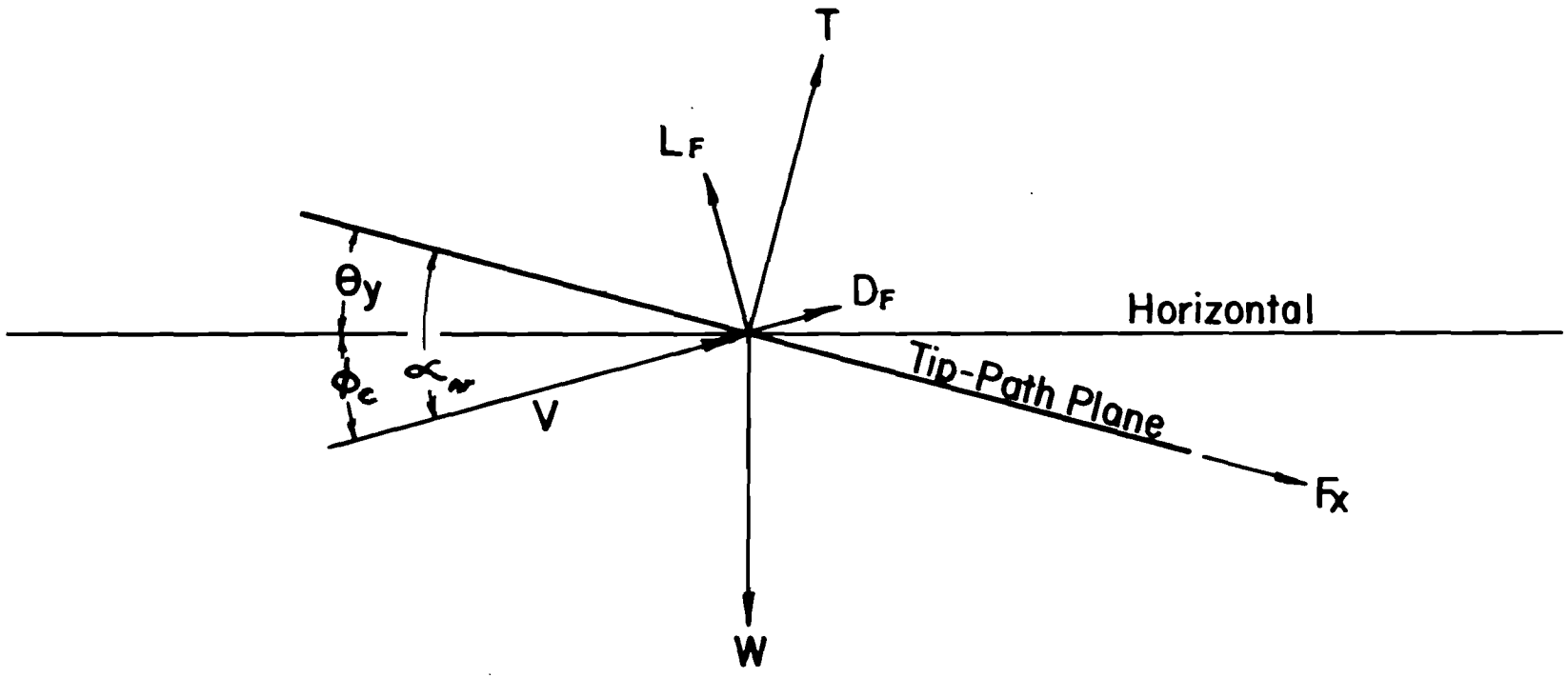

Figure 2 Forces on Rotor Hub

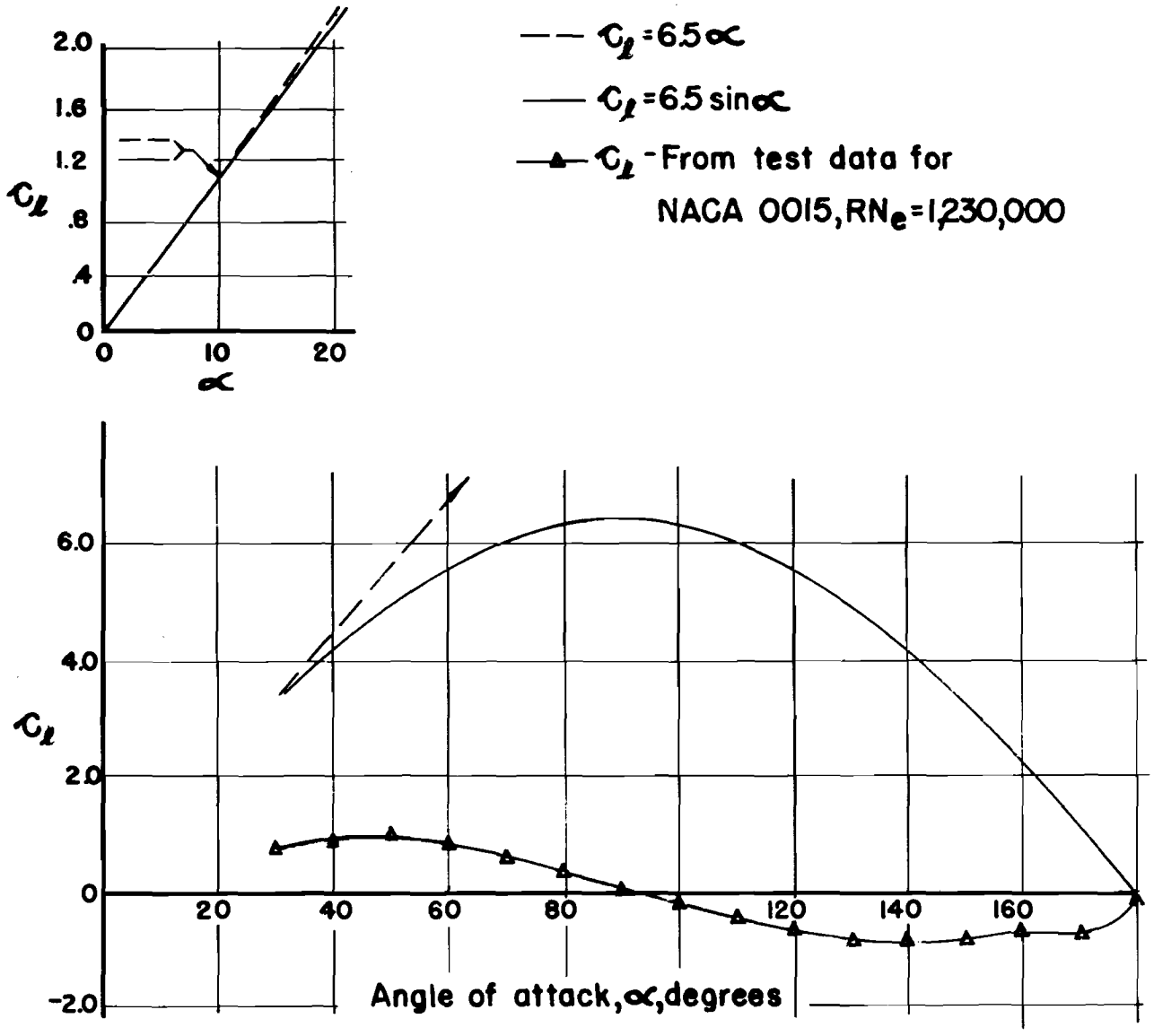

Figure 3 Comparison of Expressions for C_l

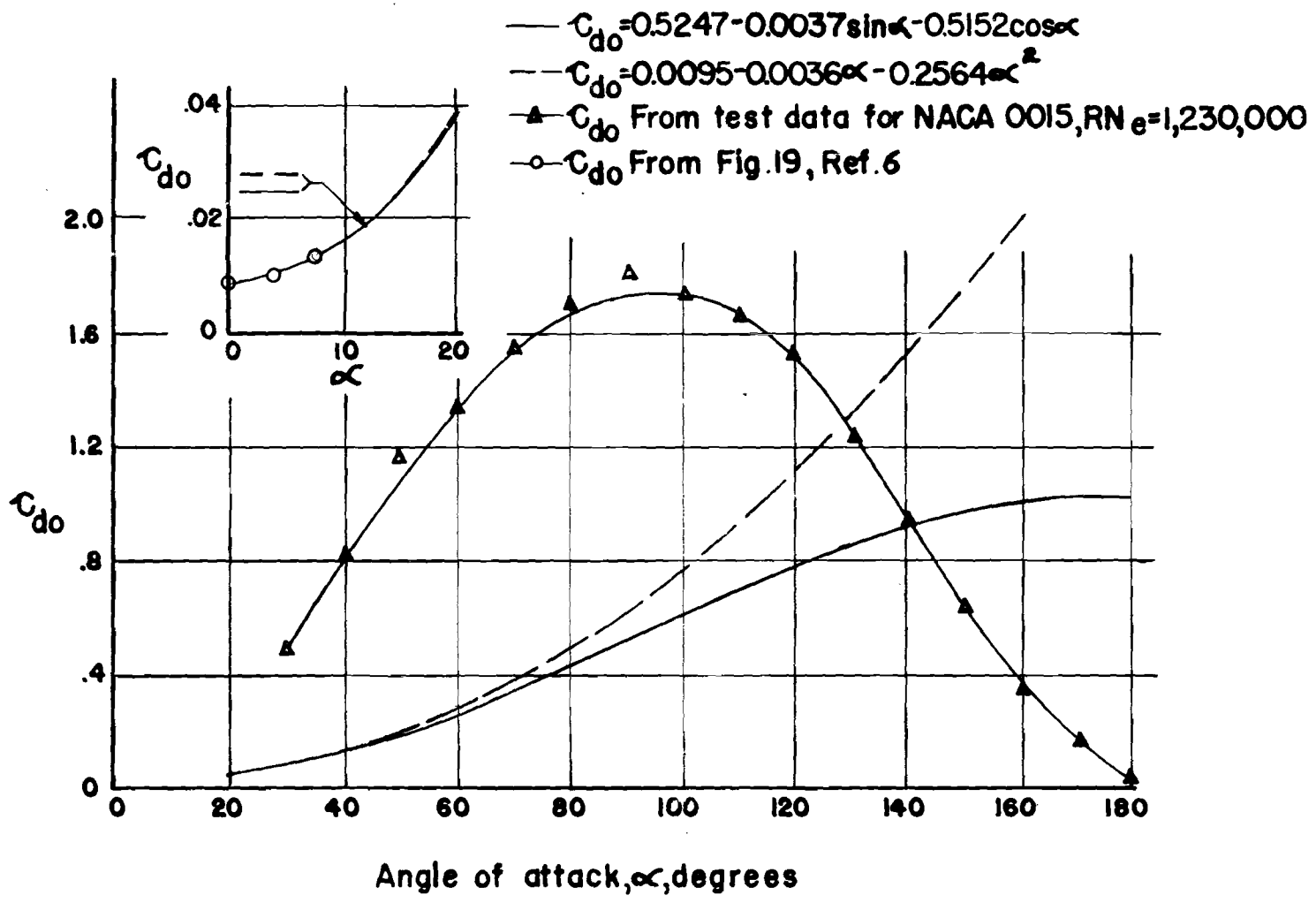

Figure 4 Comparison of Expressions for C_{do}

TABLE 1

VALUES OF σ_n FOR BLADES WITH LINEAR TAPER

Note: Interpolate for values for given t

$$\sigma_o = \frac{c_o}{\pi R}, \quad t = \frac{c_{tip}}{c_o} - 1, \quad c = c_o(1 + tx)$$

Part A for $\chi_1 = 0.15$				
	$\frac{\sigma_1}{\sigma_o}$	$\frac{\sigma_2}{\sigma_o}$	$\frac{\sigma_3}{\sigma_o}$	$\frac{\sigma_4}{\sigma_o}$
t = 0	0.8500	0.4888	0.3322	0.2499
t = -1	0.3612	0.1566	0.0823	0.0499

Part B for $\chi_1 = 0.20$				
	$\frac{\sigma_1}{\sigma_o}$	$\frac{\sigma_2}{\sigma_o}$	$\frac{\sigma_3}{\sigma_o}$	$\frac{\sigma_4}{\sigma_o}$
t = 0	0.8000	0.4800	0.3307	0.2496
t = -1	0.3200	0.1493	0.0811	0.0497

TABLE 2

COMPARISON OF EXPERIMENTAL VALUES OF α_{nr} AND C_Q WITH THOSE CALCULATED FROM APPROXIMATE BLADE-CIRCULATION EQUATIONS

Experimental Values for $C_T \approx 0.00545$

From Ref. 1. Values of f from Ref. 7

Run	α_f	f	ϕ_c	α_{nr}	C_Q	μ
7	-2.2	22.4	0	-2.08	0.000202	0.142
4	-4.5	22.7	0	-3.83	0.000244	0.189
2	-6.9	23.1	0	-5.82	0.000342	0.230
11	-10.1	24.4	-6.57	-9.97	0.000359	0.166
15	-19.4	26.4	20.80	18.77	-0.000008	0.119

Calculated Values for $a = 6.5$

Run	(2cd. appr.) μ_{nr}	(2cd. appr.) λ_{nr}	($F_x = 0$) α_{nr}	(2cd. appr.) α_{nr}	(1st. approx.) C_Q	(1st approx.) C_x	(2cd. approx) C_Q
7	0.144	-0.0241	-2.13	-2.00	0.000226	-0.0000243	0.000224
4	0.192	-0.0272	-3.88	-3.71	0.000247	-0.0000313	0.000244
2	0.235	-0.0354	-5.89	-5.58	0.000307	-0.0000602	0.000300
11	0.169	-0.0447	-9.88	-9.54	0.000349	-0.0000650	0.000343
15	0.118	0.0166	18.90	18.75	-0.000003	-0.0000279	-0.000002

Note: 2 ft.^{2} of drag area has been added to the fuselage drag area to allow for drag of C.T. rotor, camera installation, etc.

Lift of fuselage has been neglected.

Severe tip stall occurred on Run 2.

Comparison of Values of C_x and C_y

From Approximate Circulation and Blade-Element Equations ($a = 6.5$)

Run	Circulation Values (2cd. approximation)		Blade Element Values	
	C_x	C_y	C_x	C_y
7	-0.0000238	-0.000288	-0.0000256	-0.000279
4	-0.0000301	-0.000321	-0.0000351	-0.000318
2	-0.0000572	-0.000372	-0.0000754	-0.000370
11	-0.0000635	-0.000301	-0.0000549	-0.000261
15	0.0000276	-0.000283	0.0000255	-0.000308

TABLE 3 - Section 1

VALUES OF $\lambda_i = \frac{v}{\Omega R}\sqrt{\frac{2-3\mu_\alpha^2}{C_T}}$ FOR GIVEN VALUES OF

$\lambda_x = \mu_\alpha\sqrt{\frac{2-3\mu_\alpha^2}{C_T}}$ AND $\lambda_z = \frac{V\sin\alpha_\alpha}{\Omega R}\sqrt{\frac{2-3\mu_\alpha^2}{C_T}}$

Note: Values above double line are experimental, values above single line are estimated.

λ_x = / λ_z	.00	.40	.60	.80	1.00	1.20	1.40	1.60	1.80	2.00
2.40	0.960	0.740	0.580	0.481	0.457	0.433	0.410	0.390	0.371	0.349
2.20	1.14	0.88	0.68	0.543	0.509	0.476	0.444	0.418	0.392	0.369
2.00	1.36	1.07	0.82	0.630	0.574	0.526	0.484	0.450	0.418	0.389
1.80	1.65	1.34	1.03	0.767	0.659	0.585	0.529	0.483	0.445	0.410
1.60	2.26	1.81	1.42	1.000	0.769	0.654	0.577	0.518	0.472	0.432
1.40	2.44	2.05	1.77	1.220	0.896	0.727	0.627	0.550	0.496	0.452
1.20	2.24	1.88	1.65	1.25	0.976	0.789	0.668	0.582	0.520	0.470
1.00	2.01	1.72	1.52	1.21	1.000	0.824	0.698	0.613	0.539	0.485
0.80	1.80	1.56	1.39	1.15	0.984	0.833	0.713	0.621	0.552	0.494
0.60	1.60	1.41	1.27	1.07	0.947	0.820	0.712	0.625	0.556	0.500
0.40	1.42	1.28	1.16	1.00	0.897	0.792	0.698	0.619	0.554	0.500
0.20	1.25	1.15	1.06	0.924	0.842	0.756	0.677	0.606	0.547	0.494
0.00	1.10	1.02	0.96							
0.00	1.000	0.961	0.914	0.854	0.786	0.715	0.648	0.586	0.533	0.486
-0.20	0.905	0.874	0.833	0.787	0.731	0.673	0.613	0.564	0.516	0.474
-0.40	0.820	0.796	0.765	0.724	0.680	0.632	0.584	0.539	0.497	0.461
-0.60	0.744	0.725	0.699	0.668	0.630	0.592	0.551	0.513	0.477	0.443
-0.80	0.677	0.658	0.640	0.615	0.586	0.553	0.520	0.487	0.453	0.426
-1.00	0.618	0.605	0.588	0.569	0.544	0.517	0.489	0.462	0.435	0.409
-1.20	0.566	0.556	0.543	0.526	0.506	0.484	0.460	0.433	0.413	0.392
-1.40	0.521	0.512	0.501	0.488	0.472	0.453	0.433	0.413	0.394	0.374
-1.60	0.481	0.473	0.464	0.454	0.440	0.426	0.408	0.391	0.374	0.358
-1.80	0.445	0.439	0.432	0.424	0.411	0.399	0.385	0.371	0.356	0.341
-2.00	0.414	0.409	0.403	0.395	0.386	0.376	0.364	0.352	0.339	0.326
-2.40	0.362	0.358	0.355	0.350	0.342	0.334	0.327	0.318	0.308	0.298
-2.80	0.320	0.318	0.316	0.311	0.306	0.301	0.294	0.287	0.280	0.273
-3.20	0.287	0.284	0.282	0.280	0.276	0.272	0.267	0.262	0.256	0.250
-3.60	0.259	0.257	0.256	0.254	0.251	0.248	0.244	0.240	0.236	0.231
-4.00	0.236	0.235	0.234	0.233	0.230	0.227	0.225	0.223	0.221	0.214
-5.00	0.193	0.192	0.192	0.191	0.189	0.187	0.186	0.184	0.182	0.180
-6.00	0.162	0.162	0.162	0.161	0.160	0.159	0.158	0.157	0.156	0.155
-8.00	0.123	0.123	0.123	0.122	0.122	0.122	0.121	0.121	0.120	0.120
-10.00	0.100	0.100	0.100	0.100	0.099	0.099	0.099	0.098	0.098	0.097

TABLE 3 - Section 2

VALUES OF $\lambda_i = \frac{V}{\Omega R}\sqrt{\frac{2-3\mu_w^2}{C_T}}$ FOR GIVEN VALUES OF

$\lambda_x = \mu_w\sqrt{\frac{2-3\mu_w^2}{C_T}}$ AND $\lambda_z = \frac{V\sin\alpha_w}{\Omega R}\sqrt{\frac{2-3\mu_w^2}{C_T}}$

λ_x =	2.40	2.80	3.20	3.60	4.00	5.00	6.00	8.00	10.00
λ_z									
2.40	0.315	0.285	0.261	0.239	0.210	0.184	0.156	0.120	0.097
2.20	0.329	0.295	0.267	0.245	0.224	0.186	0.158	0.121	0.098
2.00	0.344	0.305	0.275	0.250	0.228	0.188	0.159	0.122	0.099
1.80	0.357	0.315	0.282	0.256	0.233	0.191	0.161	0.122	0.099
1.60	0.370	0.325	0.289	0.260	0.237	0.192	0.162	0.123	0.099
1.40	0.384	0.333	0.295	0.265	0.240	0.195	0.163	0.124	0.099
1.20	0.395	0.341	0.301	0.269	0.243	0.196	0.164	0.124	0.099
1.00	0.404	0.347	0.306	0.272	0.246	0.197	0.165	0.124	0.100
0.80	0.413	0.352	0.309	0.276	0.248	0.198	0.166	0.125	0.100
0.60	0.415	0.356	0.311	0.277	0.249	0.199	0.166	0.125	0.100
0.40	0.416	0.357	0.312	0.278	0.250	0.200	0.167	0.125	0.100
0.20	0.414	0.357	0.312	0.278	0.250	0.200	0.167	0.125	0.100
0.00									
0.00	0.410	0.354	0.310	0.278	0.250	0.200	0.167	0.125	0.100
-0.20	0.404	0.350	0.309	0.275	0.248	0.199	0.166	0.125	0.100
-0.40	0.395	0.345	0.305	0.273	0.247	0.198	0.166	0.125	0.100
-0.60	0.386	0.339	0.301	0.270	0.245	0.197	0.165	0.125	0.100
-0.80	0.374	0.331	0.296	0.267	0.242	0.196	0.165	0.125	0.100
-1.00	0.362	0.323	0.290	0.262	0.239	0.194	0.164	0.124	0.099
-1.20	0.349	0.314	0.284	0.258	0.235	0.192	0.163	0.124	0.099
-1.40	0.337	0.305	0.277	0.252	0.231	0.190	0.161	0.123	0.099
-1.60	0.325	0.296	0.270	0.247	0.227	0.188	0.160	0.122	0.099
-1.80	0.312	0.286	0.263	0.242	0.223	0.186	0.158	0.121	0.098
-2.00	0.300	0.277	0.255	0.236	0.219	0.183	0.157	0.121	0.098
-2.40	0.278	0.259	0.241	0.224	0.209	0.178	0.153	0.119	0.097
-2.80	0.258	0.242	0.227	0.213	0.200	0.172	0.149	0.117	0.096
-3.20	0.239	0.226	0.214	0.202	0.191	0.166	0.145	0.115	0.095
-3.60	0.222	0.216	0.201	0.191	0.182	0.160	0.141	0.113	0.094
-4.00	0.207	0.198	0.189	0.181	0.173	0.154	0.137	0.111	0.093
-5.00	0.175	0.170	0.164	0.159	0.155	0.139	0.127	0.105	0.089
-6.00	0.152	0.148	0.144	0.140	0.137	0.126	0.117	0.094	0.085
-8.00	0.118	0.120	0.115	0.112	0.111	0.105	0.093	0.088	0.078
-10.00	0.096	0.095	0.094	0.093	0.092	0.089	0.085	0.078	0.070

TABLE 4

VALUES OF σ_{nc} FOR BLADES WITH LINEAR TAPER, LINEAR TWIST AND x = 0.15

Note: Interpolate for values for given t first and then for values for given θ_1. Reference station for A_0 at x = 0.

$$\sigma_o = \frac{c_o}{\pi R}, \quad t = \frac{c_{tip}}{c_o} - 1, \quad c = c_o (1 + tx), \quad \theta_t = \theta_1 x$$

θ_1	$\frac{\sigma_{1c}}{\sigma_o}$		$\frac{\sigma_{2c}}{\sigma_o}$		$\frac{\sigma_{3c}}{\sigma_o}$		$\frac{\sigma_{4c}}{\sigma_o}$	
	t = 0	t = -1	t = 0	t = -1	t = 0	t = -1	t = 0	t = -1
0°	0.8500	0.3612	0.4888	0.1566	0.3322	0.0823	0.2499	0.0499
-4	0.8492	0.3611	0.4882	0.1565	0.3317	0.0822	0.2495	0.0498
-8	0.8468	0.3604	0.4864	0.1561	0.3303	0.0820	0.2483	0.0497
-12	0.8427	0.3594	0.4833	0.1555	0.3278	0.0816	0.2462	0.0494
-16	0.8371	0.3580	0.4791	0.1546	0.3244	0.0810	0.2434	0.0490
-20	0.8299	0.3562	0.4737	0.1536	0.3201	0.0803	0.2398	0.0485
-24	0.8211	0.3541	0.4671	0.1522	0.3148	0.0794	0.2354	0.0478
-28	0.8108	0.3515	0.4594	0.1507	0.3087	0.0784	0.2303	0.0471

TABLE 5

VALUES OF σ_{hs} FOR BLADES WITH LINEAR TAPER, LINEAR TWIST AND $x_1 = 0.15$

Note: Interpolate for values for given t first and then for values for given θ_1. Reference station for A_0 at x = 0.

$$\sigma_0 = \frac{c_0}{\pi R}, \quad t = \frac{c_{tip}}{c_0} - 1, \quad c = c_0 (1 + tx), \quad \theta_t = \theta_1 x$$

θ_1	$\frac{\sigma_{1s}}{\sigma_0}$		$\frac{\sigma_{2s}}{\sigma_0}$		$\frac{\sigma_{3s}}{\sigma_0}$		$\frac{\sigma_{4s}}{\sigma_0}$	
	t = 0	t = -1	t = 0	t = -1	t = 0	t = -1	t = 0	t = -1
0°	0.0000	0.0000	0.0000	0.0000	0.0000	0.0000	0.0000	0.0000
-4	-.0341	-.0109	-.0232	-.0057	-.0174	-.0035	-.0139	-.0023
-8	-.0681	-.0219	-.0463	-.0115	-.0348	-.0070	-.0279	-.0047
-12	-.1020	-.0327	-.0693	-.0172	-.0521	-.0104	-.0417	-.0070
-16	-.1356	-.0435	-.0920	-.0229	-.0692	-.0138	-.0553	-.0092
-20	-.1699	-.0531	-.1145	-.0284	-.0860	-.0173	-.0688	-.0115
-24	-.2017	-.0650	-.1367	-.0341	-.1026	-.0206	-.0820	-.0137
-28	-.2340	-.0756	-.1585	-.0396	-.1189	-.0239	-.0950	-.0159

TABLE 6

VALUES OF σ_{nc} FOR BLADES WITH LINEAR TAPER, HELICAL TWIST AND $x_1 = 0.20$

Note: Interpolate for values for given t first and then for values of given θ_T. Reference station for A_o at blade tip

$$\sigma_o = \frac{c_o}{\pi R}, \quad t = \frac{c_{tip}}{c} - 1, \quad c = c_o (1 + tx),$$

$$\theta_t = \tan^{-1} \left(\frac{1}{x} \tan \theta_T \right)$$

θ_T	$\frac{\sigma_{1c}}{\sigma_o}$		$\frac{\sigma_{2c}}{\sigma_o}$		$\frac{\sigma_{3c}}{\sigma_o}$		$\frac{\sigma_{4c}}{\sigma_o}$	
	t = 0	t = -1	t = 0	t = -1	t = 0	t = -1	t = 0	t = -1
0°	0.8000	0.3200	0.4800	0.1493	0.3307	0.0810	0.2496	0.0497
-4	0.7906	0.3144	0.4762	0.1474	0.3287	0.0803	0.2484	0.0493
-8	0.7654	0.3002	0.4651	0.1419	0.3233	0.0782	0.2451	0.0483
-12	0.7305	0.2804	0.4500	0.1351	0.3149	0.0751	0.2398	0.0468
-16	0.6907	0.2594	0.4313	0.1270	0.3042	0.0714	0.2328	0.0448
-20	0.6489	0.2385	0.4104	0.1185	0.2919	0.0674	0.2244	0.0427
-24	0.6065	0.2184	0.3882	0.1100	0.2782	0.0632	0.2151	0.0404
-28	0.5645	0.1994	0.3651	0.1016	0.2635	0.0590	0.2046	0.0379
-32	0.5231	0.1815	0.3416	0.0934	0.2481	0.0547	0.1935	0.0354

TABLE 7

VALUES OF σ_{hs} FOR BLADES WITH LINEAR TAPER, HELICAL TWIST AND $x_1 = 0.20$

Note: Interpolate for values for given t first and then for values for given θ_T. Reference station for A_o at blade tip

$$\sigma_o = \frac{c_o}{\pi R}, \quad t = \frac{c_{tip}}{c_o} - 1, \quad c = c_o (1 + tx),$$

$$\theta_t = \tan^{-1}\left(\frac{1}{x} \tan \theta_T\right)$$

θ_T	$\frac{\sigma_{1s}}{\sigma_o}$		$\frac{\sigma_{2s}}{\sigma_o}$		$\frac{\sigma_{3s}}{\sigma_o}$		$\frac{\sigma_{4s}}{\sigma_o}$	
	t = 0	t = -1	t = 0	t = -1	t = 0	t = -1	t = 0	t = -1
0	0.0000	0.0000	0.0000	0.0000	0.0000	0.0000	0.0000	0.0000
-4	-.1106	-.0553	-.0553	-.0220	-.0333	-.0103	-.0230	-.0056
-8	-.2121	-.1045	-.1076	-.0422	-.0654	-.0200	-.0454	-.0110
-12	-.3005	-.1452	-.1553	-.0596	-.0957	-.0287	-.0669	-.0160
-16	-.3761	-.1780	-.1981	-.0744	-.1237	-.0364	-.0872	-.0205
-20	-.4405	-.2044	-.2365	-.0872	-.1494	-.0431	-.1062	-.0245
-24	-.4956	-.2256	-.2701	-.0972	-.1728	-.0490	-.1239	-.0281
-28	-.5430	-.2428	-.3002	-.1060	-.1941	-.0540	-.1401	-.0313
-32	-.5838	-.2570	-.3269	-.1134	-.2134	-.0584	-.1551	-.0342

TABLE 8 - Section 1

COMPARISON OF EXPERIMENTAL AND CALCULATED VALUES OF THE PARAMETERS

FOR THOSE RUNS OF REFERENCE 1 FOR WHICH $C_T \approx 0.00545$

All Angles in Degrees, Severe Tip Stall on Run 2

	RUN 7 Level Flight at 43.7 m.p.h.			RUN 4 Level Flight at 58.6 m.p.h.			RUN 2 Level Flight at 71.7 m.p.h.		
	Exp.	Cal.	Cal.Ref.1	Exp.	Cal.	Cal.Ref.1	Exp.	Cal.	Cal.Ref.1
α_N	-2.08	-2.00		-3.83	-3.71		-5.82	-5.58	
A_0	7.11	7.42	8.5	8.17	7.94	9.3	10.10	9.11	11.3
a_1	2.92	2.88	2.9	4.37	3.84	4.0	6.08	5.03	5.5
a_0	8.16	8.38	7.9	8.30	8.31	8.2	8.67	8.44	8.4
b_1	3.24	2.89	2.4	3.30	3.14	2.7	3.93	3.48	3.2
a_2	0.24	0.18	0.15	0.35	0.28	0.26	0.46	0.42	0.40
b_2	0.00	-0.04	-0.05	-0.08	-0.09	-0.10	-0.11	-0.17	-0.18
C_Q	0.000202	0.000213		0.000244	0.000240		0.000342	0.000310	
δ_0	-7.45	-7.58		-8.83	-8.50		-12.50	-11.02	
E_1' *	0.41	0.51		0.54	0.58		0.67	0.69	
F_1' *	-0.21	-0.07		-0.18	-0.10		-0.27	-0.17	
C_x		-0.000026			-0.000035			-0.000075	
C_y		-0.000279			-0.000318			-0.000370	
$\text{Tan}^{-1}\left(\frac{C_x}{2C_T}\right)$		-0.13			-0.18			-0.43	
θ_x		0.02			0.00			0.11	
θ_y		-2.00			-3.71			-5.58	
$\left(\frac{\Delta C_T}{C_T}\right)_{3rd.}$		0.012			0.027			0.049	

* Note: Mechanical Input Subtracted

TABLE 8 - Section 2

COMPARISON OF EXPERIMENTAL AND CALCULATED VALUES OF THE PARAMETERS

FOR THOSE RUNS OF REFERENCE 1 FOR WHICH $C_T \approx 0.00545$

All Angles in Degrees, Severe Tip Stall on Run 2

	RUN 11 525 f.p.m. climb at 51.8 m.p.h.			RUN 15 1260 f.p.m. autorotative descent at 37.7 m.p.h.		
	Exp.	Cal.	Cal.Ref.1	Exp.	Cal.	Ca.Ref.1
α_v	-9.97	-9.54		18.77	18.75	
A_o	10.00	9.50	11.0	3.40	3.57	5.0
a_1	4.23	3.81	3.93	1.07	1.76	1.85
a_o	9.15	8.64	8.34	7.55	7.88	7.53
b_1	3.56	2.93	1.87	2.86	2.85	1.23
a_2	0.33	0.24	0.19	0.08	0.12	0.08
b_2	-0.10	-0.08	-0.10	-0.02	-0.00	-0.03
C_Q	0.000359	0.000334		-0.000008	-0.000019	
s_o	-13.03	-11.88		-0.03	0.67	
E_1 *	0.70	0.53		0.21	0.47	
F_1 *	-0.37	-0.16		0.26	0.03	
C_x		-0.000055			0.000026	
C_y		-0.000261			-0.000308	
$\text{Tan}^{-1}\left(\frac{C_x}{2C_T}\right)$		-0.29			0.27	
θ_x		0.78			-1.49	
θ_y		-2.98			-2.05	
$\left(\frac{\Delta C_T}{C_T}\right)_{3rd.\ har.}$		0.020			0.007	

* Note: Mechanical Input Subtracted